www.elsevier.com/locate/yjtbi

The influence of cytokinin-auxin cross-regulation on cell-fate determination in *Arabidopsis thaliana* root development

Daniele Muraro, Helen Byrne, John King, Ute Voß, Joseph Kieber, Malcolm Bennett

PII: S0022-5193(11)00253-0
DOI: doi:10.1016/j.jtbi.2011.05.011
Reference: YJTBI6475

To appear in: *Journal of Theoretical Biology*

Received date: 19 October 2010
Revised date: 6 May 2011
Accepted date: 10 May 2011

Cite this article as: Daniele Muraro, Helen Byrne, John King, Ute Voß, Joseph Kieber and Malcolm Bennett, The influence of cytokinin-auxin cross-regulation on cell-fate determination in *Arabidopsis thaliana* root development, *Journal of Theoretical Biology*, doi:10.1016/j.jtbi.2011.05.011

The influence of cytokinin-auxin cross-regulation on cell-fate determination in *Arabidopsis thaliana* root development

Daniele Muraro[a,*], Helen Byrne[a,b], John King[a,b], Ute Voß[a], Joseph Kieber[c], Malcolm Bennett[a]

[a] *Centre for Plant Integrative Biology, School of Biosciences, University of Nottingham, Sutton Bonington Campus, Loughborough LE12 5RD, UK*
[b] *School of Mathematical Sciences, University of Nottingham, University Park, Nottingham NG7 2RD, UK*
[c] *Department of Biology, The University of North Carolina at Chapel Hill, Chapel Hill, North Carolina 27599-3280*

Abstract

Root growth and development in *Arabidopsis thaliana* are sustained by a specialised zone termed the meristem, which contains a population of dividing and differentiating cells that are functionally analogous to a stem cell niche in animals. The hormones auxin and cytokinin control meristem size antagonistically. Local accumulation of auxin promotes cell division and the initiation of a lateral root primordium. By contrast, high cytokinin concentrations disrupt the regular pattern of divisions that characterises lateral root development, and promote differentiation. The way in which the hormones interact is controlled by a genetic regulatory network. In this paper, we propose a deterministic mathematical model to describe this network and present model simulations that reproduce the experimentally observed effects of cytokinin on the expression of auxin regulated genes. We show how

*Corresponding author. *E-mail address*: Daniele.Muraro@nottingham.ac.uk

auxin response genes and auxin efflux transporters may be affected by the presence of cytokinin. We also analyse and compare the responses of the hormones auxin and cytokinin to changes in their supply with the responses obtained by genetic mutations of *SHY2*, which encodes a protein that plays a key role in balancing cytokinin and auxin regulation of meristem size. We show that, although *shy2* mutations can qualitatively reproduce the effect of varying auxin and cytokinin supply on their response genes, some elements of the network respond differently to changes in hormonal supply and to genetic mutations, implying a different, general response of the network. We conclude that an analysis based on the ratio between these two hormones may be misleading and that a mathematical model can serve as a useful tool for stimulate further experimental work by predicting the response of the network to changes in hormone levels and to other genetic mutations.

Keywords:
Lateral root development, cytokinin-auxin cross-regulation, mathematical modelling

1. Introduction

Plants have evolved so that they can efficiently adapt their growth patterns in response to environmental stimuli. A well-balanced pattern of roots and shoots is crucial for optimal uptake of nutrients, light and water. New organ formation is typically restricted to the post-embryonic stage, whereas tissue regeneration can occur over a long time period, in some cases centuries. This activity is sustained by plant stem cells and is regulated by complex interactions between different hormones.

Hormonal signalling is essential for controlling organ growth and differentiation. Two of the most influential plant hormones are auxin and cytokinin.

Auxin coordinates organ growth by promoting cell division through its interactions with other hormones such as cytokinin, gibberellin and ethylene. For simplicity, in this paper we will focus on the cross-talk between auxin and cytokinin. Unlike auxin, cytokinin downregulates cell division in roots, and upregulates cell division in shoots. A common analysis of the balance of these two hormones is based on changes in their ratio. A high auxin-to-cytokinin concentration ratio promotes root formation, whereas a low ratio promotes shoot development [1]. Interactions between these two hormones are also believed to guide important patterning processes in shoots such as *apical dominance*, the phenomenon whereby one meristem dominates another [1]. In roots, the balance between auxin and cytokinin is known to control the size of the *meristem*, a population of undifferentiated cells located near the root cap. Auxin is transported by PIN efflux transporters from the shoot and tends to accumulate in the meristematic region sustaining cell division and root growth [2]. Cytokinin is produced in a wide range of organs and cell types. In roots, the main sites of cytokinin biosynthesis are located in the elongation zone, a region above the meristem, and in the columella, a tissue in the root cap [3], [4]. The auxin-to-cytokinin ratio is then likely to vary in different root tissues, being probably higher in the meristem than in the elongation zone. Of particular interest here, cytokinin is known to prevent the formation of the auxin gradient that is required to pattern the lateral root primordium [5]; nevertheless, it is not clear how this phenomenon occurs, and mathematical models may be helpful to draw new hypotheses.

Some of the subcellular interactions between auxin and cytokinin are known [3]. In particular, a cytokinin-mediated pathway interacts with an auxin-coordinated feedback loop, provoking an antagonistic and reciprocal adaptation of the two hormone responses.

Several mathematical models have been proposed to investigate the mechanism of auxin transport during lateral root development (see for example [6,7]). However, these models do not take into account the cross-talk between auxin and cytokinin and its influence on the response to an auxin stimulus. A subcellular mathematical model of the auxin feedback loop, and an investigation of its dynamics and response to auxin supply have been proposed in [8]. For a particular range of parameters the solutions evolve to a stable limit cycle. The predicted oscillatory behaviour has been interpreted by the authors as a possible cause of the oscillations in the Aux/IAA response of a protoxylem cell located in the basal meristem, as suggested in [9].

In this paper, we extend the model of the auxin network developed in [8] by introducing the cytokinin pathway and investigating its influence on the cross-talk with the auxin pathway. We present simulations which show that the application of cytokinin may disrupt the oscillatory behaviour found in [8], with an increase in cytokinin supply shown to be responsible for a reduction both in the auxin response and in the expression of auxin efflux transporters, the PIN proteins. These results are consistent with the experimental observations reported in [5] and provide preliminary validation of some of our model predictions, confirming the important role of cytokinin in auxin regulation.

We analyse the network response to SHY2 gain- and loss-of-function mu-

tants, and we compare their effects with those caused by enhancing, respectively, the cytokinin and auxin supply. We predict that the loss-of-function mutant qualitatively reproduces the effects of an increase in auxin supply on the auxin and cytokinin reponses, whereas the gain-of-function mutant emulates the effects of an increase in cytokinin supply. In our simulations, this analogy does not extend to all elements of the network, suggesting that the system responses to changes in hormone levels and genetic mutations are not identical. The opposite qualitative responses in some of these elements could be experimentally validated by measuring steady state levels of mRNA and proteins among wild type plants, SHY2 mutants, and plants with altered auxin and cytokinin levels. We conclude that our model can stimulate further experimental work by predicting the response of the network to perturbations of its elements.

The paper is structured as follows. In section 2 we review the relevant experimental evidence and summarise the known auxin-cytokinin interactions. In section 3 we introduce our mathematical model. In section 4 we present our simulation results and compare them with experimental observations. Finally, in section 5, we summarise and interpret our findings and outline directions for future research.

2. Biological background

The early events in the patterning of lateral roots are organized via a signalling cascade whose initial stimulus comes from the localized accumulation of auxin. We summarise below the main events associated with lateral root initiation at this early developmental stage, focusing on the roles of auxin

and cytokinin and their interactions.

2.1. Lateral root initiation

Within the main root, lateral roots are initiated in a transition zone that is located between the elongation zone, which contains differentiated cells, and the meristem, a tissue of undifferentiated cells that sustains root growth. Lateral roots of *Arabidopsis thaliana* are generated exclusively in the pericycle, a cylinder of cells that constitutes the external part of the stele, inside the endodermis. In particular, the pericycle founder cells are located opposite the xylem, whose basic function is to transport water and nutrients (see Figure 1).

FIGURE 1

When auxin levels are elevated, an auxin-dependent pre-initiation event primes the pericycle founder cells for lateral root initiation. The auxin reporter DR5::GUS appears to be localized both longitudinally and radially in two short strands just above the meristem (see Figures 1a and 1b) [9]. The founder cells then divide anticlinally and periclinally, generating a dome-shaped primordium that eventually emerges from the main root (Figure 1c). For a review of lateral root development see, for example, [10].

Priming is associated with the formation of a local, spatial gradient of auxin, whose maximum is located in the founder cells, and is dependent on auxin transport by efflux transporters known as PIN proteins [11]. The local auxin response has been found to oscillate with a period of approximatively 15 hours in [9], and of about 6 hours in [12]. The peak concentration corre-

lates with the formation of a lateral root [9, 12]. The oscillations may be due to fluctuations in auxin redistribution within the root apex [9], or to periodic cellular dynamics [12, 13]. The results presented in [12] are interpreted by the authors to suggest that an oscillatory network, located in a region between the basal meristem and elongation zone, is the endogenous developmental mechanism triggering periodic branching and bending in the *Arabidopsis* root. The authors also highlight similarities with the segmentation clock in vertebrates, where somite patterning depends on a clock-and-wavefront mechanism.

At the cellular level the auxin response is controlled by the activation of the *Aux/IAA* genes, a family of genes that are rapidly induced in response to auxin (indole-3-acetic acid, IAA). Most of the *Aux/IAA* genes have binding sites in their promoter region to which Auxin Response Factors (ARFs) can bind, activating or inhibiting Aux/IAA transcription [14, 15]. We assume that ARF proteins exist as monomers and dimers and that both act as transcription factors. *In vitro* studies suggest that the repression associated with the negative auxin feedback loop happens only when ARFs are present and that it is implemented by Aux/IAA-ARF heterodimers [29, 30]. The resulting complex acts as a transcription factor repressing *Aux/IAA* genes. Such transcriptional regulation, of a gene by its translational proteins, constitutes a negative feedback loop. The feedback loop is disrupted by auxin in the following way. Auxin binds to its receptor (TIR1) which interacts with the cullin AtCUL1 and a SKP1-like protein to form the auxin-SCF-TIR1 complex. This complex targets the Aux/IAA protein for proteolysis and degradation [18, 19, 20].

A mathematical model of this gene regulatory network was developed in [8]. For a specific parameter regime, the model was shown to undergo a Hopf bifurcation at a critical value of auxin supply. The periodicity of the resulting oscillatory solutions is coordinated by the feedback loop as follows. Free ARF proteins compete with Aux/IAA proteins in the regulation of Aux/IAA transcription. When the levels of Aux/IAA proteins fall, the concentration of free ARFs increases, enhancing Aux/IAA transcription and translation. The subsequent accumulation of Aux/IAA protein stimulates the formation of Aux/IAA-ARF complexes. The direct repression of the *Aux/IAA* gene, and the indirect reduction in ARF activation, diminishes Aux/IAA mRNA and protein concentrations. The concentration of free ARFs then increases, and so the oscillations persist. This oscillatory network may represent a simplified version of the complex oscillatory network proposed in [12]. The periodicity of the network response in a group of cells may be due to the synchronization of oscillating gene networks in each cell, by analogy with the synchronization of the oscillatory subcellular networks which are analysed in the literature on somitogenesis modelling (see for example [21,22]).

Cytokinins exert a negative regulatory effect on lateral root development [5]. For example, targeted expression of a gene responsible for cytokinin biosynthesis (*IPT5*) revealed that the xylem pole cells are sensitive to cytokinin. Higher concentrations of cytokinin disrupt the regular pattern of division that characterises lateral root primordium organization. In [5] it was observed that cytokinin disrupts the expression of *PIN* genes in the founder cells and prevents the formation of an auxin gradient. In particular, the expression of PIN1,2,3,4 and 7 was reduced in cytokinin treated plants.

Interactions between cytokinin and auxin in many cases are mutually antagonistic. In the root, both hormones activate their own response genes, and repress the response of their antagonist (see Figure 2). In addition, the auxin response is regulated by the negative feedback loop described above, and the cytokinin response is negatively regulated by feedback via the type-A ARRs.

Auxin and cytokinin are also known to control each others biosynthesis: auxin represses cytokinin biosynthesis in seedlings treated with NAA in a dose-dependent manner [1] and upregulates *IPT5* and *IPT7* genes [4], whereas cytokinin promotes auxin biosynthesis [23]. These processes occur via different pathways which are not well characterised, and affect only the supply of auxin and cytokinin, which are initial perturbations in our model. Since we want to analyse the network response to changes in hormone supplies, we neglect the effects of auxin and cytokinin biosynthesis, and we treat their supply rates as inputs to the network.

Details of the interactions between cytokinin and auxin are described in the next section.

FIGURE 2

2.2. Cytokinin-auxin signalling interactions

Cytokinin perception at the external part of the cell membrane initiates signalling between the cytokinin response and the auxin mediated Aux/IAA negative feedback loop.

Cytokinin is perceived by AHK receptors at the cell membrane which

autophosphorylate in response to cytokinin binding. The AHK phosphoryl group is then transferred to the Arabidopsis His Phosphotransfer Proteins (AHPs) within the cytoplasm, which, in turn, transfer it to the type A and B Arabidopsis Response Regulators (ARR-A and ARR-B). Phosphorylation promotes ARR-A and ARR-B function, respectively repressing and activating the cytokinin response (CR). ARR-B can also intensify Aux/IAA transcription, thus reinforcing the Aux/IAA feedback loop [24].

Auxin can diffuse within the plasma membrane or be actively transported into the cell, by AUX/LAX influx transporters, and out of the cell, by PIN proteins [27]. A member of the Aux/IAA proteins family, SHY2 (Short Hypocotyl 2), is known to downregulate PIN1,3,7, and thereby to block auxin efflux transport [24]. Auxin indirectly controls meristem growth by degrading SHY2 protein and derepressing PIN activity via the feedback loop described in section 2.1. High concentrations of auxin release the ARF oligomers by degrading the Aux/IAA proteins, inducing the expression of auxin-response genes. An unidentified auxin signalling component, which is dependent on auxin response (AR) and ARF activation, promotes the expression of ARR-A, negatively regulating the cytokinin response (CR) [3].

Crosstalk between the two signalling pathways can be summarised as follows. Auxin activates its own response, which, in turn, promotes ARR-A transcription by regulating cytokinin signalling pathway; on the other hand, cytokinin activates ARR-B transcription factors which promote the expression of SHY2 and affect auxin signalling pathway. SHY2 activity is crucial to the balance between cell division and differentiation because of its role in negatively regulating PIN activity. Cytokinin mediated transcription of

SHY2 downregulates PIN proteins, obstructing auxin flux and promoting cell differentiation. Conversely, auxin-mediated ubiquitination of SHY2 sustains PIN activity and cell division.

3. Mathematical model

The mathematical model that we propose extends the negative feedback loop model of Aux/IAA developed in [8]. In order to minimise the complexity of the network and to model partially known reactions, we group in a single variable species that are known to act in a similar way. For example, we will consider only one member of the 29 *Aux/IAA* genes [25,26], which we assume to be *Shy2* or another possible Aux/IAA member that may interact with cytokinin. We will describe separately auxin and cytokinin mediated regulation, and then highlight the coupling between the two networks. In section 3.1 we describe the Aux/IAA model, introduce the coupling with cytokinin response genes, and explain how they regulate the auxin response genes and PIN efflux transporters. Likewise, in section 3.2 we present our model for cytokinin-mediated regulation of auxin and cytokinin response genes. The model equations are obtained primarily by applying the law of mass action, while transcription is modelled by Michaelis-Menten kinetics (i.e. assuming rapid protein-DNA binding). In what follows, we will denote chemical concentrations by square brackets and rates of association, dissociation, and modification by the subscripts a, d, m respectively. The cellular reactions and the species included in our model are summarised in Figure 3 and in Tables 1 and 2.

FIGURE 3

3.1. Auxin-mediated regulation

We assume that auxin is synthesized and degraded at the constant rates ω_{Aux} and μ_{Aux}, so that

$$\emptyset \xrightarrow{\omega_{\text{Aux}}} \text{Aux} \xrightarrow{\mu_{\text{Aux}}} \emptyset.$$

Additionally, auxin binds to TIR1, forming the Aux:TIR1 complex so that

$$\text{Aux} + \text{TIR1} \underset{k_d}{\overset{k_a}{\rightleftharpoons}} \text{Aux:TIR1},$$

where k_a, k_d represent the association and dissociation rates. The Aux:TIR1 complex targets IAA_p for ubiquitination by forming an intermediate complex Aux:TIR1:IAA whose dissociation results in the formation of the ubiquitin-tagged protein IAA^*, which degrades at rate μ_{IAA^*}. This process is governed by the following reactions:

$$\text{Aux:TIR1} + \text{IAA}_p \underset{l_d}{\overset{l_a}{\rightleftharpoons}} \text{Aux:TIR1:IAA},$$

$$\text{Aux:TIR1:IAA} \xrightarrow{l_m} \text{Aux:TIR1} + \text{IAA}^*,$$

$$\text{IAA}^* \xrightarrow{\mu_{\text{IAA}^*}} \emptyset,$$

with association, dissociation and ubiquitination rates l_a, l_d, l_m. ARF monomers can homodimerise and bind Aux/IAA proteins:

$$\begin{aligned} &\text{ARF} + \text{ARF} \underset{q_d}{\overset{q_a}{\rightleftharpoons}} \text{ARF}_2, \\ &\text{IAA}_p + \text{ARF} \underset{p_d}{\overset{p_a}{\rightleftharpoons}} \text{ARF:IAA}. \end{aligned} \tag{1}$$

In (1), ARF_2, ARF:IAA are respectively the ARF homodimer and heterodimer, whereas the q_a, p_a, q_d, p_d represent the association and dissociation rates.

While ARR-B and ARF are known to have different binding sites [15,28], it is not yet known whether their crosstalk occurs in competition or cooperation. We have used our mathematical model to test both variants and found that, assuming cooperation, the responses of auxin and cytokinin to changes in cytokinin supply were incompatible with what is observed experimentally. We interpret this result as indicating that ARR-B and ARF compete in regulating Aux/IAA transcription and, henceforth, we make this assumption in our model.

Transcription of *Aux/IAA* gene is controlled by four transcription factors: the ARF monomer, the ARF homodimer, the ARF:IAA complex and the phosphorylated ARR-B protein (ARR-Bph) [29,30,24]. We model Aux/IAA transcription assuming Michaelis-Menten kinetics and by introducing the functions $F^{(1)}_{\text{ARF}}, F^{(1)}_{\text{ARF}_2}, F^{(1)}_{\text{ARR-Bph}}$ to represent the probability that a particular activator is bound to the gene, where

$$F^{(1)}_{\text{ARF}}(t) := \frac{[\text{ARF}]}{\theta_{\text{ARF}}} \Big/ Den_1(t),\ F^{(1)}_{\text{ARF}_2}(t) := \frac{[\text{ARF}_2]}{\theta_{\text{ARF}_2}} + \frac{[\text{ARF}]^2}{\psi_{\text{ARF}}} \Big/ Den_1(t),$$
$$F^{(1)}_{\text{ARR-Bph}}(t) := \frac{[\text{ARR-Bph}]}{\theta_{\text{ARR-Bph}}} \Big/ Den_1(t),$$

where

$$Den_1(t) := 1 + \frac{[\text{ARF}]}{\theta_{\text{ARF}}} + \Big(\frac{[\text{ARF}_2]}{\theta_{\text{ARF}_2}} + \frac{[\text{ARF}]^2}{\psi_{\text{ARF}}}\Big) + \Big(\frac{[\text{ ARF:IAA}]}{\theta_{\text{ARF:IAA}}} + \frac{[\text{ARF}][\text{IAA}_p]}{\psi_{\text{ARF:IAA}}} + \frac{[\text{ARR-Bph}]}{\theta_{\text{ARR-Bph}}}\Big),$$

and where $\theta_{\mathrm{ARF}},\ \theta_{\mathrm{ARF}_2},\ \psi_{\mathrm{ARF}},\ \theta_{\mathrm{ARF:IAA}},\ \psi_{\mathrm{ARF:IAA}},\ \theta_{\mathrm{ARR\text{-}Bph}}$ are the binding thresholds of the relevant protein or protein complex. The maximum transcription rates are denoted by $\lambda^{(1)}_{\mathrm{ARF}}, \lambda^{(1)}_{\mathrm{ARF}_2}, \lambda_{\mathrm{ARR\text{-}Bph}}$, and the rates of Aux/IAA mRNA turnover and translation are respectively μ_{IAA_m} and δ_{IAA_p}. Transcription and translation reactions are thus modelled by

$$\emptyset \xrightarrow{\lambda^{(1)}_{\mathrm{ARF}} F^{(1)}_{\mathrm{ARF}} + \lambda^{(1)}_{\mathrm{ARF}_2} F^{(1)}_{\mathrm{ARF}_2} + \lambda_{\mathrm{ARR\text{-}Bph}} F^{(1)}_{\mathrm{ARR\text{-}Bph}}} \mathrm{IAA}_m,$$

$$\mathrm{IAA}_m \xrightarrow{\mu_{\mathrm{IAA}_m}} \emptyset,\ \mathrm{IAA}_m \xrightarrow{\delta_{\mathrm{IAA}_p}} \mathrm{IAA}_m + \mathrm{IAA}_p.$$

We group together the auxin-response genes in a single gene expressing AR_m. Transcription of AR_m is enhanced by ARF monomers and homodimers and is modelled by the functions:

$$F^{(2)}_{\mathrm{ARF}}(t) := \frac{[\mathrm{ARF}]}{\theta_{\mathrm{ARF}}} \Big/ Den_2(t),\ F^{(2)}_{\mathrm{ARF}_2}(t) := \frac{[\mathrm{ARF}_2]}{\theta_{\mathrm{ARF}_2}} + \frac{[\mathrm{ARF}]^2}{\psi_{\mathrm{ARF}}} \Big/ Den_2(t),$$

where

$$Den_2(t) := Den_1(t) - \frac{[\mathrm{ARR\text{-}Bph}]}{\theta_{\mathrm{ARR\text{-}Bph}}}.$$

Denoting the maximum transcription rates by $\lambda^{(2)}_{\mathrm{ARF}}, \lambda^{(2)}_{\mathrm{ARF}_2}$, and the rates of AR mRNA turnover and translation respectively by μ_{AR_p} and δ_{AR_p}, one has

$$\emptyset \xrightarrow{\lambda^{(2)}_{\mathrm{ARF}} F^{(2)}_{\mathrm{ARF}} + \lambda^{(2)}_{\mathrm{ARF}_2} F^{(2)}_{\mathrm{ARF}_2}} \mathrm{AR}_m \xrightarrow{\mu_{\mathrm{AR}_m}} \emptyset,$$

$$\mathrm{AR}_m \xrightarrow{\delta_{\mathrm{AR}_p}} \mathrm{AR}_m + \mathrm{AR}_p,\ \mathrm{AR}_p \xrightarrow{\mu_{\mathrm{AR}_p}} \emptyset.$$

AR_p promotes transcription of ARR-A, which in turn represses cytokinin response genes. Consequently, activation of an auxin response negatively regulates the cytokinin response (see section 3.2).

The SHY2 protein is a member of the Aux/IAA family, which is known to downregulate PIN1,3,7. In consequence, Aux:TIR1-mediated degradation of SHY2 sustains PIN activity. In order to be consistent with experimental observations of SHY2 gain- and loss-of-function mutants we suppose that downregulation of PIN by SHY2 is an indirect effect of ARF activation (see section 4.3 for a discussion). In our notation SHY2 is included in the Aux/IAA group and PIN proteins are lumped together in a single protein. Gene transcription of PIN is thus modelled by the regulatory functions $F^{(2)}_{\mathrm{ARF}}$ and $F^{(2)}_{\mathrm{ARF}_2}$. Using similar notation for the rates of PIN mRNA transcription, turnover and translation, as used above, for AR mRNA we have

$$\emptyset \xrightarrow{\lambda^{(2)}_{\mathrm{ARF}} F^{(2)}_{\mathrm{ARF}} + \lambda^{(2)}_{\mathrm{ARF}_2} F^{(2)}_{\mathrm{ARF}_2}} \mathrm{PIN}_m \xrightarrow{\mu_{\mathrm{PIN}_m}} \emptyset,$$

$$\mathrm{PIN}_m \xrightarrow{\delta_{\mathrm{PIN}_p}} \mathrm{PIN}_m + \mathrm{PIN}_p, \ \mathrm{PIN}_p \xrightarrow{\mu_{\mathrm{PIN}_p}} \emptyset.$$

Applying the law of mass balance to the components of the regulatory net-

work, we obtain the following system of ordinary differential equations:

$$
\begin{aligned}
&\frac{d[\mathrm{IAA}_m]}{dt} = \lambda^{(1)}_{\mathrm{ARF}} F^{(1)}_{\mathrm{ARF}}(t) + \lambda^{(1)}_{\mathrm{ARF}_2} F^{(1)}_{\mathrm{ARF}_2}(t) + \lambda_{\text{ARR-Bph}} F^{(1)}_{\text{ARR-Bph}}(t) - \mu_{\mathrm{IAA}_m}[\mathrm{IAA}_m],\\
&\frac{d[\mathrm{IAA}_p]}{dt} = \delta_{\mathrm{IAA}_p}[\mathrm{IAA}_m] - l_a[\mathrm{IAA}_p][\text{Aux:TIR1}] + l_d[\text{Aux:TIR1:IAA}] - p_a[\mathrm{IAA}_p][\mathrm{ARF}]\\
&+ p_d[\text{ARF:IAA}],\\
&\frac{d[\text{Aux:TIR1}]}{dt} = k_a[\text{Aux}][\text{TIR1}] - k_d[\text{Aux:TIR1}] + (l_d + l_m)[\text{Aux:TIR1:IAA}]\\
&- l_a[\text{Aux:TIR1}][\mathrm{IAA}_p],\\
&\frac{d[\text{Aux:TIR1:IAA}]}{dt} = -(l_d + l_m)[\text{Aux:TIR1:IAA}] + l_a[\text{Aux:TIR1}][\mathrm{IAA}_p],\\
&\frac{d[\mathrm{IAA}^*]}{dt} = l_m[\text{Aux:TIR1:IAA}] - \mu_{\mathrm{IAA}^*}[\mathrm{IAA}^*],\\
&\frac{d[\text{ARF:IAA}]}{dt} = p_a[\mathrm{ARF}][\mathrm{IAA}_p] - p_d[\text{ARF:IAA}],\\
&\frac{d[\mathrm{ARF}_2]}{dt} = q_a[\mathrm{ARF}]^2 - q_d[\mathrm{ARF}_2],
\end{aligned}
\tag{2}
$$

$$
\begin{aligned}
&\frac{d[\text{Aux}]}{dt} = \omega_{\text{Aux}} + k_d[\text{Aux:TIR1}] - k_a[\text{Aux}][\text{TIR1}] - \mu_{\text{Aux}}[\text{Aux}],\\
&\frac{d[\mathrm{PIN}_m]}{dt} = \lambda^{(2)}_{\mathrm{ARF}} F^{(2)}_{\mathrm{ARF}}(t) + \lambda^{(2)}_{\mathrm{ARF}_2} F^{(2)}_{\mathrm{ARF}_2}(t) - \mu_{\mathrm{PIN}_m}[\mathrm{PIN}_m],\\
&\frac{d[\mathrm{PIN}_p]}{dt} = \delta_{\mathrm{PIN}_p}[\mathrm{PIN}_m] - \mu_{\mathrm{PIN}_p}[\mathrm{PIN}_p],\\
&\frac{d[\mathrm{AR}_m]}{dt} = \lambda^{(2)}_{\mathrm{ARF}} F^{(2)}_{\mathrm{ARF}}(t) + \lambda^{(2)}_{\mathrm{ARF}_2} F^{(2)}_{\mathrm{ARF}_2}(t) - \mu_{\mathrm{AR}_m}[\mathrm{AR}_m],\\
&\frac{d[\mathrm{AR}_p]}{dt} = \delta_{\mathrm{AR}_p}[\mathrm{AR}_m] - \mu_{\mathrm{AR}_p}[\mathrm{AR}_p].
\end{aligned}
$$

The above equations extend the auxin model in [8], by taking into account PIN and AR transcription and translation and Aux/IAA transcription via $\lambda_{\text{ARR-Bph}} F^{(1)}_{\text{ARR-Bph}}$. We assume that the total concentrations of TIR1 and

ARF are constant. Thus, the levels of [TIR1] and [ARF] can be calculated from the conservation laws

$$[\text{TIR1}]_T = [\text{TIR1}] + [\text{Aux:TIR1}] + [\text{Aux:TIR1:IAA}],$$

$$[\text{ARF}]_T = [\text{ARF}] + [\text{ARF:IAA}] + 2[\text{ARF}_2],$$

where $[\text{TIR1}]_T, [\text{ARF}]_T$ are the assumed constant total concentrations of the complexes bound to TIR1 and ARF respectively. The parameter values for a dimensionless version of the model are stated in Appendix A. When solving equations (2) all variables are initially set to zero, except for [Aux], whose value at $t = 0$ is a prescribed, typical auxin concentration that is normalised so that $[\text{Aux}](t = 0) = 1$ in the dimensionless model. In Table 1 we summarise the species involved in auxin regulation.

TABLE 1

3.2. Cytokinin-mediated regulation

As for the auxin model, we assume that cytokinin is synthesized at a constant rate ω_{Ck} and degraded at rate μ_{Ck}, so that

$$\emptyset \xrightarrow{\omega_{\text{Ck}}} \text{Ck} \xrightarrow{\mu_{\text{Ck}}} \emptyset.$$

Cytokinin may bind reversibly to the AHK receptor, which autophosphorylates, finally forming the complex Ck:AHKph. In our model, we simplify this process by assuming that binding and phosphorylation are synchronous via the interaction between cytokinin and the variable AHKph

$$\text{Ck} + \text{AHKph} \underset{r_d}{\overset{r_a}{\rightleftharpoons}} \text{Ck:AHKph},$$

with association and dissociation rates r_a, r_d. ARR-A transcription is activated by unknown auxin response signalling components which may depend on ARF regulation. Here we assume that it is activated by the AR group via Michaelis-Menten kinetics and hence we model ARR-A transcription using

$$F_{\mathrm{AR}}(t) := \frac{\frac{[\mathrm{AR}_p]}{\theta_{\mathrm{AR}}}}{1 + \frac{[\mathrm{AR}_p]}{\theta_{\mathrm{AR}}}},$$

where θ_{AR} is the binding threshold for AR. Denoting the maximum transcription rate by λ_{AR}, and the rates of ARR-A mRNA turnover and translation by $\mu_{\text{ARR-A}_p}$ and $\delta_{\text{ARR-A}_p}$, we deduce that the reactions associated with transcription and translation can be written as

$$\emptyset \xrightarrow{\lambda_{\mathrm{AR}} F_{\mathrm{AR}}} \text{ARR-A}_m \xrightarrow{\mu_{\text{ARR-A}_m}} \emptyset,$$

$$\text{ARR-A}_m \xrightarrow{\delta_{\text{ARR-A}_p}} \text{ARR-A}_m + \text{ARR-A}_p,$$

$$\text{ARR-A}_p \xrightarrow{\mu_{\text{ARR-A}_p}} \emptyset.$$

The complex Ck:AHKph transfers its phosphoryl group via the AHPs to ARR-A and ARR-B protein. In our model we simplify this regulation by neglecting the role of the AHPs, and considering a reversible reaction between the Ck:AHKph complex and the ARRs.

$$\text{Ck:AHKph} + \text{ARR-A}_p \underset{s_d}{\overset{s_a}{\rightleftharpoons}} \text{Ck:AHK} + \text{ARR-Aph},$$

$$\text{Ck:AHKph} + \text{ARR-B}_p \underset{u_d}{\overset{u_a}{\rightleftharpoons}} \text{Ck:AHK} + \text{ARR-Bph},$$

with association and dissociation rates s_a, s_d, u_a, u_d. Phosphorylated ARR-A (ARR-Aph) represses cytokinin response genes whereas phosphorylated ARR-B (ARR-Bph) activates them. As in the auxin model, we group together the cytokinin response genes and view them as a single generic gene

producing the protein Cytokinin Response, which we denote by CR. The transcription of this gene is governed by Michaelis-Menten kinetics, via the function $F^{(2)}_{\text{ARR-Bph}}(t)$, which is defined as follows:

$$F^{(2)}_{\text{ARR-Bph}}(t) := \frac{\frac{[\text{ARR-Bph}]}{\theta_{\text{ARR-Bph}}}}{1 + \frac{[\text{ARR-Aph}]}{\theta_{\text{ARR-Aph}}} + \frac{[\text{ARR-Bph}]}{\theta_{\text{ARR-Bph}}}},$$

where $\theta_{\text{ARR-Aph}}, \theta_{\text{ARR-Bph}}$ are the binding thresholds of ARR-A and ARR-B. Denoting the maximum transcription rate by $\lambda^{(2)}_{\text{ARR-Bph}}$, and the rates of ARR-A mRNA turnover and translation by μ_{CR_p} and δ_{CR_p}, we deduce that the reactions for transcription and translation can be written as

$$\emptyset \xrightarrow{\lambda^{(2)}_{\text{ARR-Bph}} F^{(2)}_{\text{ARR-Bph}}} \text{CR}_m \xrightarrow{\mu_{\text{CR}_m}} \emptyset,$$

$$\text{CR}_m \xrightarrow{\delta_{\text{CR}_p}} \text{CR}_m + \text{CR}_p, \ \text{CR}_p \xrightarrow{\mu_{\text{CR}_p}} \emptyset.$$

Phosphorylated ARR-B also activates Aux/IAA transcription, strengthening the Aux/IAA feedback loop, and downregulating auxin response genes. In this way, cytokinin-mediated phosphorylation represses the auxin response (see section 3.1). By appealing to the principle of mass balance, we deduce that cytokinin-mediated regulation may be modelled by the following system

of ordinary differential equations:

$$\frac{d[\mathrm{CR}_m]}{dt} = \lambda^{(2)}_{\text{ARR-Bph}} F^{(2)}_{\text{ARR-Bph}}(t) - \mu_{\mathrm{CR}_m}[\mathrm{CR}_m],$$
$$\frac{d[\mathrm{CR}_p]}{dt} = \delta_{\mathrm{CR}_p}[\mathrm{CR}_m] - \mu_{\mathrm{CR}_p}[\mathrm{CR}_p],$$
$$\frac{d[\text{AHKph}]}{dt} = r_d[\text{Ck:AHKph}] - r_a[\text{AHKph}][\text{Ck}],$$
$$\frac{d[\text{Ck}]}{dt} = \omega_{\text{Ck}} - \mu_{\text{Ck}}[\text{Ck}] + r_d[\text{Ck:AHKph}] - r_a[\text{Ck}][\text{AHKph}],$$
$$\frac{d[\text{ARR-Bph}]}{dt} = u_a[\text{Ck:AHKph}][\text{ARR-B}_p] - u_d[\text{Ck:AHK}][\text{ARR-Bph}],$$
$$\frac{d[\text{ARR-Aph}]}{dt} = s_a[\text{ARR-A}_p][\text{Ck:AHKph}] - s_d[\text{ARR-Aph}][\text{Ck:AHK}],$$
$$\frac{d[\text{ARR-A}_m]}{dt} = \lambda_{\text{AR}} F_{\text{AR}}(t) - \mu_{\text{ARR-A}_m}[\text{ARR-A}_m],$$
$$\frac{d[\text{ARR-A}_p]}{dt} = \delta_{\text{ARR-A}_p}[\text{ARR-A}_m] - \mu_{\text{ARR-A}_p}[\text{ARR-A}_p] - s_a[\text{Ck:AHKph}][\text{ARR-A}_p]$$
$$+ s_d[\text{Ck:AHK}][\text{ARR-Aph}]. \tag{3}$$

We assume that the total concentrations of ARR-B protein ($[\text{ARR-B}_p]_T$), the AHK receptor ($[\text{AHK}]_T$), and the phosphoryl group PH ($[\text{PH}]_T$) are constant. Thus, the values of $[\text{ARR-B}_p]$, [Ck:AHK] and [Ck:AHKph] can be determined from the conservation laws

$$[\text{ARR-B}_p]_T = [\text{ARR-B}_p] + [\text{ARR-Bph}],$$
$$[\text{AHK}]_T = [\text{AHKph}] + [\text{Ck:AHK}] + [\text{Ck:AHKph}],$$
$$[\text{PH}]_T = [\text{AHKph}] + [\text{ARR-Aph}] + [\text{ARR-Bph}] + [\text{Ck:AHKph}],$$

where $[\text{ARR-B}]_T, [\text{AHK}]_T, [\text{PH}]_T$ represent the total concentrations of the complexes bound respectively to ARR-B, the phosphoryl group, and the AHK receptor. The parameter values for a dimensionless version of the model are stated in Appendix A. When solving equations (3) all variables

are initially set to zero, except for [Ck] and [AHKph], whose value at $t = 0$ is a prescribed, typical concentration that is normalised so that $[\mathrm{Ck}](t = 0) = 1$ and $[\mathrm{AHKph}](t = 0) = 1$ in the dimensionless model. In Table 2 we summarise the species involved in cytokinin regulation.

TABLE 2

3.3. Auxin-cytokinin interaction

Our full model of auxin and cytokinin cross-regulation comprises equations (2) for the auxin submodel and (3) for the cytokinin submodel. The submodels are coupled as follows.

Application of auxin triggers the degradation of Aux/IAA by ubiquitination via its binding with TIR1. The reduction in levels of the heterodimer ARF:IAA stimulates the transcription of auxin response genes. The increase in AR promotes ARR-A transcription and increases the levels of phosphorylated ARR-A (ARR-Aph), which in turn represses cytokinin response genes.

Application of cytokinin facilitates the phosphorylation of ARR-B via its binding with the AHKph receptor. ARR-Bph acts as a transcription factor both of cytokinin response and of Aux/IAA genes. The increase in Aux/IAA protein intensifies the concentration of the ARF:IAA heterodimer. Finally, the higher amount of ARF:IAA provokes a stronger repression of auxin response genes.

A dimensionless version of our model is presented in Appendix A, together with the default parameters and initial conditions. In the next section

we analyse and compare the simulations of the rescaled model with experimental data.

4. Model dynamics and comparison with experiments

In this section we numerically investigate the dynamics of the dimensionless model defined by the rescaled versions of equations (2) and (3) (see equations (A.5) and (A.8) in Appendix A). We show how cytokinin regulation affects the dynamics of the Aux/IAA feedback loop, and we compare our results with experimental observations. In section 4.1 we focus on the parameter values for which the auxin model exhibits limit cycle behaviour, basing on [8], and show how the oscillatory dynamics are disrupted by cytokinin regulation. In section 4.2 we discuss the response and recovery times for an auxin supply in the presence of cytokinin. Finally, in section 4.3 we focus on the steady state solutions and their sensitivity to changes in the supply of auxin (α_{Aux} in (A.1)) and cytokinin (α_{Ck} in (A.6)). We model the SHY2 gain- and loss-of-function mutants, and we consider how well these mutants mimic the effects of increasing α_{Aux} and α_{Ck}.

4.1. Periodic dynamics

Extensive simulations of equations (A.5), (A.8) have been performed using the *Mathematica* routine *NDSolve*, which solves a wide range of ordinary differential equations as well as many partial differential equations by automatically selecting an appropriate integration method. These methods include Runge Kutta, non-stiff Adams, stiff Gear method. Other options for numerical algorithms and their accuracy are described in the Help entry of *NDSolve*. At long time the model evolves to either a stable steady state or

a stable limit cycle and the outcome depends crucially on the levels of auxin and cytokinin regulation. Numerical software is available in the literature to construct bifurcation diagrams (see for example [31,32]). Here, we have used the *XPP* routine *AUTO* [32] to analyse the bifurcation structure of the system defined by the equations (A.5), (A.8).

In Figure 4 we present two bifurcation diagrams showing how the long time Aux/IAA protein dynamics vary with the supply rate of auxin (α_{Aux}) and the rescaled parameter $\alpha_{\text{ARR-B}}$, describing the concentration of ARR-B relative to the total concentration of the AHK receptor (for the definition of $\alpha_{\text{ARR-B}}$ see (A.6)). The system undergoes a Hopf bifurcation as α_{Aux} increases through a critical value and as $\alpha_{\text{ARR-B}}$ decreases through a threshold value. The bifurcation structure of equations (A.5), (A.8) in the $(\alpha_{\text{Aux}}, \alpha_{ARR-B})$ plane is presented in Figure 5. The mechanism described above may be interpreted as follows. The site of cytokinin biosynthesis is mainly located in the differentiation zone [3] where, according to the scenario proposed in [13], the cells stop oscillating and, depending on the phase of the cycle, they may be capable of forming lateral roots. Cytokinin may be responsible for disrupting the internal clock of cells in these regions.

We now investigate how auxin oscillations influence the cytokinin response, and conversely the effects of cytokinin on auxin-mediated oscillations and PIN concentration. In Figure 6 on the left we present a typical limit-cycle solution generated using our model. For low levels of cytokinin and ARR-B, the oscillations caused by the Aux/IAA feedback loop persist and similar, but time-delayed, oscillations are induced in the cytokinin response. In this regime, auxin levels continue to oscillate, maintaining the potential

for periodic lateral root formation under low levels of endogeneous cytokinin in the founder cells [9, 5].

In Figure 6 on the right we show how the phase and amplitude of the oscillations varies with the rescaled ARF dimerization parameter q_a (defined in (A.3)). We assume that when the association rate is smaller than the dissociation rate ($q_a < q_d$) the majority of ARFs that are present are monomers. Model simulations show that decreasing the association rate causes the amplitudes of the auxin and cytokinin oscillations to increase and decrease respectively, while the phase difference reduces.

In Figure 7a we show how the steady-state levels of PIN protein vary with the cytokinin supply (α_{Ck}). In [5] the authors reported a reduction in PIN expression when cytokinin supply was enhanced. The decrease in the concentration of PIN auxin efflux facilitators as α_{Ck} increases, as predicted by our model, is consistent with experimental observations [5].

PIN mediated reflux is presumably involved in generating the auxin maximum in the protoxylem cells adjacent to the pericycle cells [9]. According to our model, the periodic formation of the auxin maximum may be related to the periodicity of the concentration of its efflux transporters. In Figures 7b and 7c we show how the introduction of cytokinin may disrupt the oscillations in a PIN efflux transporter.

FIGURE 4

FIGURE 5

FIGURE 6

FIGURE 7

4.2. Time dependent solutions

In [8] the response of the Aux/IAA feedback loop model to perturbations away from its large-time state was analysed by exposing the system to either a continuous source of auxin or an auxin pulse. Experimental observations show that an increase in auxin triggers Aux/IAA mRNA levels to rise monotonically [33]. In [8] this response could be obtained with the Aux/IAA feedback loop model. In our model, the application of cytokinin causes an increase in Aux/IAA expression, thus enhancing the effect of auxin-treatment, while also restoring the qualitative behaviour of the Aux/IAA feedback loop and agreement with the experiments.

In [8] it is assumed that the rescaled concentrations of SCF-TIR1 (α_{TIR1} in (A.1)) and ARF (α_{ARF} in (A.1)) are likely to vary in different plant tissues. This variability may be due, for example, to the regulation of other hormones that are not uniformly distributed in all plant tissues. These quantities can influence the time that the Aux/IAA feedback loop needs to respond to, and recover from, an auxin pulse. The response and recovery times proved to be insensitive to variations of two orders of magnitudes in α_{ARF} when $\alpha_{\mathrm{TIR1}} \gg 1$, and to increase linearly with α_{TIR1} [8]. In our model, the application of cytokinin, although strengthening the feedback loop, does not significantly alter the times of response to and recovery from an auxin pulse.

4.3. Mutants

SHY2 plays a key role in balancing auxin- and cytokinin-mediated regulation. ARR1, a member of the ARR-B family, binds directly to, and activates the SHY2 promoter in the transition zone [24]. SHY2 transcription is enhanced by cytokinin in wild type roots, while no effects have been detected in *arr-1* mutant roots [24]. In [33] the response of 14 members of the family of *Aux/IAA* genes to auxin was analysed. The response of most genes to continuous treatment with exogenous auxin was rapid (within 4 to 30 minutes), leading to increases in mRNA levels of around 4− to 25−fold. An increase in either cytokinin or auxin enhances transcription of members of the Aux/IAA family. This behaviour is illustrated in Figures 8 and 9, where we show how the steady states of the Aux/IAA group depend on auxin and cytokinin supply. An increase in auxin supply triggers an increase in Aux/IAA transcription but a decrease in its translation, whereas an increase in the application of cytokinin stimulates both transcription and translation of Aux/IAA. The opposite effect of auxin and cytokinin supply on the translation of Aux/IAA is then responsible for the antagonistic effect of these two hormones on transcription and translation of auxin response genes and cytokinin response genes, as shown in Figures 8 and 9 for auxin and cytokinin response proteins (respectively AR_p and CR_p). Hence, a decrease in auxin supply should not be considered to be equivalent to an increase in the supply of cytokinin, and any analysis based on the ratio of these two hormones may be misleading. The detailed mechanism that leads to this antagonism is described later in this section when we analyse the response of the network to changes in the supply of auxin and cytokinin.

Confirmation of the central role of SHY2 comes from the analysis of genetic mutations. The *shy2-31* loss-of-function mutant prevents SHY2 from binding with ARFs, whereas the *shy2-2* gain-of-function mutant inhibits the ubiquitination of SHY2 by blocking binding with the Aux:TIR1 complex. In [34] the *shy2-31* loss-of-function mutant was shown to produce larger root meristems. This increase in cellular division is also seen following application of auxin. In contrast, the *shy2-2* gain-of-function mutant mimics the effect of cytokinin application by triggering smaller meristems.

To gain insight into the impact that these mutants have on other network variables, we investigate the sensitivity of the steady-state solutions to variation in the supply rates of auxin and cytokinin. We then compare these results to those obtained for the gain- and loss-of-function mutants. We model the mutants by decreasing the association rates of the reactions that they hinder. In particular, we model a loss-of-function and a gain-of-function mutant respectively by reducing the rescaled parameters l_a and p_a (defined in (A.2) and (A.3)). We suppose that the mimicking effect of an increase of auxin concentration is an increase in the concentration of AR_p and a decrease in that of CR_p. Similarly we say that a response to a stimulus mimics the response to cytokinin if there is a decrease in AR_p and an increase in CR_p. In Figure 8 we show how the steady states of Aux/IAA mRNA and protein (IAA_m, IAA_p), phosphorylated ARRs of type A and B (ARR-Aph, ARR-Bph), and auxin and cytokinin response (AR_p, CR_p) vary with α_{Aux} and p_a.

An increase in α_{Aux} promotes Aux/IAA ubiquitination and, thereby, reduces Aux/IAA levels. The corresponding rise of free ARFs enhances not

only Aux/IAA transcription but also AR transcription and translation. The increase in AR concentration stimulates ARR-A transcription and translation. Therefore a higher concentration of ARR-A removes the phosphoryl group from the cytokinin-AHK-ph complex, enhancing the concentration of ARR-Aph. Since, the total concentration of the phosphoryl group is constant, an increase in ARR-Aph leads to a decrease in ARR-Bph concentration. Simulations which consider what may be more physically realistic conditions, by relaxing the assumption that the total concentration of the phosphoryl group is constant, are qualitatively similar to those presented above. For these reasons, we retained simplifying the assumption of constancy of phosphoryl groups, since it enables to reduce the number of differential equations in our model (by applying the associated conservation laws). Now, ARR-Aph and ARR-Bph respectively repress and activate the cytokinin response. The increase in the concentration of the repressor and the decrease in that of the activator cause a reduction in transcription and translation of cytokinin response genes (CR_m, CR_p).

A decrease in p_a causes an increase in free ARF concentrations and, in contrast to what is observed when α_{Aux} increases, in free IAA_p. The higher concentration of free ARF enhances the transcription and translation of auxin. The increase in AR_p then stimulates, via the mechanism described above, an increase in ARR-A, leading to an increase in ARR-Aph, a decrease in ARR-Bph, and a subsequent decrease in CR_p.

In Figure 9 we perform a similar analysis, in this case focusing on the response to changes in α_{Ck} and l_a. An increase in α_{Ck} increases the concentration of the cytokinin-AHK-ph complex. Although the total concen-

tration of the phosphoryl group is constant, the greater availability of a larger amount of the cytokinin-AHK-ph complex increases the concentration of the phosphoryl groups available for transfer to ARR-A and ARR-B. Increased phosphorylation leads to a higher concentration of both ARR-Aph and ARR-Bph. An increase in cytokinin response is obtained if the following condition is true

$$[\text{ARR-Bph}] < \theta_{\text{ARR-Aph}} + [\text{ARR-Aph}]. \tag{4}$$

For consistency with experimental observations, we assume that (4) is fulfilled.

The increase in ARR-Bph stimulates Aux/IAA transcription and translation, which, in turn, causes an increase in the concentration of the ARF-Aux/IAA complex, a reduction in the concentration of free ARF, and subsequently the transcription and translation of auxin response genes.

A decrease in l_a reduces degradation via ubiquitination of Aux/IAA protein, increasing its concentration and that of the Aux/IAA-ARF complex. The reduction in free ARF diminishes Aux/IAA transcription, in contrast to what was observed by increasing α_{Ck}, and decreases AR_p. The lower concentration of AR_p reduces expression of ARR-A and, again in contrast to what was predicted by increasing α_{Ck}, a lower concentration of ARR-Aph. The enhanced availability of the phosphoryl group in the cytokinin-AHK-ph complex triggers an increase in ARR-Bph, and ultimately a stronger cytokinin response.

We have shown that, under the assumptions of our model, the impact of the response genes on an increase in auxin and cytokinin supply is qualitatively similar to that of loss- and gain-of-function mutants. Thus, the

influence of the mutants on hormonal response genes mimics the action of hormonal supply. Nevertheless, not all elements of the network respond in the same way to the different stimuli. The Aux/IAA protein concentration decreases following the application of auxin, whereas it increases in the loss-of-function mutant. Aux/IAA mRNA transcription is strengthened by increasing the cytokinin supply thereby strengthening the feedback loop, but it is reduced by the gain-of-function mutant. Finally, the concentration of phosphorylated ARR-A is enhanced by an increase in cytokinin supply, but suppressed by the gain-of-function mutant. Therefore, the effect of the mutants is similar to changes in hormonal supply in a limited sense, i.e. the influence on the response genes, whereas there are subtle differences in their action on the other elements of the network.

The predicted response of the network to the simulated *shy2-2* gain-of-function mutant is confirmed by experimental observations in which PIN mRNA levels were found to be low in such mutants [24]. The increase in PIN mRNA and protein levels in the simulated *shy2-31* loss-of-function mutant may be responsible for the increase in the meristem size described in [24].

In Figure 10a we show the effect on the Aux/IAA steady states of simultaneously increasing the auxin and cytokinin supplies while holding the auxin-to-cytokinin concentration ratio constant. The cytokinin pathway upregulates Aux/IAA transcription, whereas the auxin pathway degrades Aux/IAA protein which represses its own gene. Since both hormones trigger a positive effect on Aux/IAA mRNA, the increase of both hormones, under this condition on the hormonal ratio, still causes an increase in Aux/IAA expression. Changes in the responses of other elements of the network may be due to the

nonlinearity of their interactions.

In Figure 10b and 10c we show how PIN mRNA steady states vary in response to changes in l_a and p_a. A decrease in l_a reduces PIN mRNA levels, whereas PIN expression is enhanced, decreasing the value of p_a. Both effects are consistent with the experimental observations mentioned above.

FIGURE 8

FIGURE 9

FIGURE 10

5. Discussion

The fate of lateral root founder cells is regulated antagonistically by auxin and cytokinin. The cross-regulation of the two hormones controls the formation and maintenance of the main root transition zone, where lateral root priming occurs, and the establishment of an auxin gradient that is required to pattern the primordium. We have proposed a mathematical model of this hormonal interaction, which generalises the Aux/IAA feedback loop model developed in [8].

The system was found to undergo Hopf bifurcations as we varied the relative concentrations of auxin and ARR-B, whose activation is triggered by cytokinin-mediated phosphorylation. Conversely, cytokinin regulation did not appear to influence auxin response in the absence of ARR-B, a result

which is consistent with experimental observations of ARR1 mutant roots [24]. In the limit cycle regime, the Aux/IAA feedback loop induces oscillations in cytokinin and the cytokinin response. A sufficiently large increase in the concentration of ARR-B disrupts the oscillations, in which case the system evolves to a stable steady state.

A high concentration of cytokinin reduces PIN mRNA expression, as experimentally observed in [5], and disrupts the cell's internal clock. This effect may provide a possible mechanism by which to identify those cells which are capable of forming lateral roots, as proposed in [13].

There is experimental evidence that SHY2 (Aux/IAA) transcription is enhanced by the application of auxin and cytokinin, [33, 3]. Conversely, in our simulations, translation is increased by cytokinin, and weakened by auxin. In fact, auxin disrupts the negative feedback loop, promoting ubiquitination of the Aux/IAA proteins, whereas cytokinin increases its strength. These differences are responsible for the antagonistic influence of auxin and cytokinin on auxin response genes. Therefore, when studying the feedback mechanism it is not sufficient to analyse just the ratio of these two hormones.

We have investigated the response of the network to an increase in auxin and cytokinin supply and to SHY2 (Aux/IAA) gain-of-function and loss-of-function mutants, and we have compared our theoretical results with experimental observations, see [3] and references therein. In our model, these mutants mimic the effects of cytokinin and auxin application, saying that the response to a stimulus mimics the effect of a hormone supply if there is an increase in the transcription of its response genes, and a decrease in the expression of the response genes of its antagonist hormone. On the other

hand, the response of some variables to hormonal stimulation differs from the response of the corresponding mutant. Therefore, the network response to hormone application and SHY2 mutations are not equivalent and could be experimentally tested by comparing changes in steady state levels of mRNA and proteins among wild type plants, SHY2 mutants, and plants with altered auxin and cytokinin levels.

We conclude that the model we have developed represents a useful tool for stimulating further experimental work enabling us to investigate in more detail the dynamic response of the network to changes in hormone levels and to genetic mutations.

Appendix A. Rescaling

In order to obtain a dimensionless model, we rescale equations (2), (3). We will consider the ratios $1/l_m$ and $1/\mu_{\mathrm{IAA}_m}$ to be representative of the timescale for degradation of Aux/IAA protein and mRNA concentrations. A summary of mRNA and protein turnover rates for several Aux/IAA family members can be found in [8]. A key parameter for the Aux/IAA feedback loop model is $\epsilon = \mu_{\mathrm{IAA}_m}/l_m$, i.e. the ratio of the timescale of ubiquitination to that of gene expression. The value of ϵ is known for some Aux/IAAs [8] and can vary in the range $\epsilon = 0.03 - 0.44$. We describe separately the rescaling associated with the auxin and cytokinin response. The rescaling of the Aux/IAA model is the same as that used in [8] with the addition of AR and PIN transcriptions and translations. We present it here for completeness.

Rescaling of auxin submodel

Since data are available for Aux/IAA mRNA concentrations in response to auxin [33], we consider a dimensionless time $\bar{t}$ based on the timescale for Aux/IAA mRNA degradation $(\mu_{\mathrm{IAA}_m})^{-1}$

$$\bar{t} \equiv \mu_{\mathrm{IAA}_m} t.$$

This scaling leads us to define the following ratios for the timescale of AR and PIN protein degradation to that of gene expression

$$\epsilon_{\mathrm{AR}} \equiv \mu_{\mathrm{AR}_m}/\mu_{\mathrm{AR}_p}, \qquad \epsilon_{\mathrm{PIN}} \equiv \mu_{\mathrm{PIN}_m}/\mu_{\mathrm{PIN}_p}.$$

In addition, it is convenient to introduce the following dimensionless constants of proportionality:

$$\tau_{\mathrm{AR}} \equiv \epsilon_{\mathrm{AR}}/\epsilon, \qquad \tau_{\mathrm{PIN}} \equiv \epsilon_{\mathrm{PIN}_m}/\epsilon.$$

Aux/IAA transcription is negatively regulated by Aux/IAA protein via the heterodimerization with ARF. We scale the rate of Aux/IAA transcription, δ_{IAA_p}, relative to the rate of Aux/IAA protein ubiquitination, l_m, introducing

$$\phi_{\mathrm{IAA}_p} \equiv \delta_{\mathrm{IAA}_p}/l_m$$

to represent the strength of the negative feedback loop, and similarly define

$$\phi_{\mathrm{AR}_p} \equiv \delta_{\mathrm{AR}_p}/\mu_{\mathrm{AR}_p}, \qquad \phi_{\mathrm{PIN}_p} \equiv \delta_{\mathrm{PIN}_p}/\mu_{\mathrm{PIN}_p},$$

by replacing the ubiquitination rate with the protein degradation rates. We consider $O(\lambda^{(1)}_{\mathrm{ARF}_2}/\mu_{\mathrm{IAA}_m})$ as an estimate for the maximum steady state concentration of Aux/IAA mRNA, in the absence of Aux/IAA protein negative

regulation and assuming $\lambda^{(1)}_{\mathrm{ARF}_2} \gg \lambda^{(1)}_{\mathrm{ARF}}, \lambda_{\text{ARR-Bph}}$, [8]. We define the rescaled dimensionless concentration of IAA_m basing it on $\frac{\lambda^{(1)}_{\mathrm{ARF}_2}}{\mu_{\mathrm{IAA}_m}} \cdot \frac{l_m}{\delta_{\mathrm{IAA}_p}}$

$$[\overline{\mathrm{IAA}_m}] \equiv \frac{\mu_{\mathrm{IAA}_m}\delta_{\mathrm{IAA}_p}}{\lambda^{(1)}_{\mathrm{ARF}_2} l_m}[\mathrm{IAA}_m].$$

In this way, ϕ_{IAA_p} represents the maximum rate of Aux/IAA transcription in the dimensionless system. Likewise, we define the scaling for AR_m and PIN_m

$$[\overline{\mathrm{AR}_m}] \equiv \frac{\mu_{\mathrm{IAA}_m}\delta_{\mathrm{AR}_p}}{\lambda^{(1)}_{\mathrm{ARF}_2}\mu_{\mathrm{AR}_p}}[\mathrm{AR}_m], \qquad [\overline{\mathrm{PIN}_m}] \equiv \frac{\mu_{\mathrm{IAA}_m}\delta_{\mathrm{PIN}_p}}{\lambda^{(2)}_{\mathrm{ARF}_2}\mu_{\mathrm{PIN}_p}}[\mathrm{PIN}_m].$$

We nondimensionalize ARF and TIR1 concentrations with typical total concentrations $[\mathrm{ARF}^{\ddagger}]_T$ and $[\mathrm{TIR1}^{\ddagger}]_T$

$$[\overline{\mathrm{ARF}}] \equiv [\mathrm{ARF}]/[\mathrm{ARF}^{\ddagger}]_T, \qquad [\overline{\mathrm{TIR1}}] \equiv [\mathrm{TIR1}]/[\mathrm{TIR1}^{\ddagger}]_T.$$

It is then convenient to scale similarly the complexes

$$([\overline{\mathrm{ARF{:}IAA}}], [\overline{\mathrm{ARF}_2}]) \equiv ([\mathrm{ARF{:}IAA}], [\mathrm{ARF}_2])/[\mathrm{ARF}^{\ddagger}]_T,$$
$$([\overline{\mathrm{Aux{:}TIR1}}], [\overline{\mathrm{Aux{:}TIR1{:}IAA}}]) \equiv ([\mathrm{Aux{:}TIR1}], [\mathrm{Aux{:}TIR1{:}IAA}])/[\mathrm{TIR1}^{\ddagger}]_T,$$
$$([\overline{\mathrm{IAA}_p}], [\overline{\mathrm{IAA}^*}], [\overline{\mathrm{AR}_p}], [\overline{\mathrm{PIN}_p}]) \equiv ([\mathrm{IAA}_p], [\mathrm{IAA}^*], [\mathrm{AR}_p], [\mathrm{PIN}_p])/[\mathrm{TIR1}^{\ddagger}]_T.$$

The concentration of free auxin is based on the representative concentration $[\mathrm{Aux}^{\ddagger}]$

$$[\overline{\mathrm{Aux}}] \equiv [\mathrm{Aux}]/[\mathrm{Aux}^{\ddagger}].$$

From these scalings we get the dimensionless parameters

$$\alpha_{\mathrm{ARF}} \equiv [\mathrm{ARF}]_T/[\mathrm{ARF}^{\ddagger}]_T, \qquad \alpha_{\mathrm{TIR1}} \equiv [\mathrm{TIR1}]_T/[\mathrm{TIR1}^{\ddagger}]_T,$$
$$\alpha_{\mathrm{Aux}} \equiv \omega_{\mathrm{Aux}}/(\mu_{\mathrm{Aux}}[\mathrm{Aux}^{\ddagger}]), \tag{A.1}$$

representing the relative concentrations of ARF and TIR1, and the relative rate of auxin supply. We also obtain the dimensionless parameters

$$\eta_{\text{Aux:TIR1}} \equiv [\text{TIR1}^{\ddagger}]_T/[\text{Aux}^{\ddagger}], \qquad \eta_{\text{ARF:IAA}} \equiv [\text{ARF}^{\ddagger}]_T/[\text{TIR1}^{\ddagger}]_T$$

that represent the auxin-TIR1 and the ARF-TIR1 concentration ratios. We base the dimensionless association and dissociation constants involved in Aux/IAA protein ubiquitination on the ubiquitination rate l_m, namely

$$\bar{k}_a \equiv (k_a[\text{Aux}^{\ddagger}])/l_m, \qquad \bar{k}_d \equiv k_d/l_m, \qquad \bar{l}_a \equiv (l_a[\text{TIR1}^{\ddagger}]_T)/l_m, \qquad \bar{l}_d \equiv l_d/l_m. \tag{A.2}$$

ARF association and dissociation rates are based on Aux/IAA mRNA degradation

$$\bar{p}_a \equiv (p_a[\text{TIR1}^{\ddagger}]_T)/\mu_{\text{IAA}_m}, \qquad \bar{p}_d \equiv p_d/\mu_{\text{IAA}_m}, \qquad \bar{q}_a \equiv (q_a[\text{ARF}^{\ddagger}]_T)/\mu_{\text{IAA}_m},$$
$$\bar{q}_d \equiv q_d/\mu_{\text{IAA}_m}. \tag{A.3}$$

Auxin degradation is based on Aux/IAA mRNA degradation, whereas tagged Aux/IAA protein is based on the ubiquitination rate

$$\bar{\mu}_{\text{Aux}} \equiv \mu_{\text{Aux}}/\mu_{\text{IAA}_m}, \qquad \bar{\mu}_{\text{IAA}^*} \equiv \mu_{\text{IAA}^*}/l_m.$$

From the scaling of ARF, TIR1 and their complexes, it is convenient to define the dimensionless protein-DNA binding concentration thresholds as follows

$$\bar{\theta}_{\text{ARF}} \equiv \theta_{\text{ARF}}/[\text{ARF}^{\ddagger}]_T, \qquad \bar{\theta}_{\text{ARF}_2} \equiv \theta_{\text{ARF}_2}/[\text{ARF}^{\ddagger}]_T,$$
$$\bar{\theta}_{\text{ARF:IAA}} \equiv \theta_{\text{ARF:IAA}}/[\text{ARF}^{\ddagger}]_T, \qquad \bar{\theta}_{IAA} \equiv \theta_{IAA}/[\text{TIR1}^{\ddagger}]_T,$$
$$\bar{\theta}_{\text{AR}} \equiv \theta_{\text{AR}}/[\text{TIR1}^{\ddagger}]_T, \qquad \bar{\psi}_{\text{ARF:IAA}} \equiv \psi_{\text{ARF:IAA}}/([\text{ARF}^{\ddagger}]_T[\text{TIR1}^{\ddagger}]_T),$$
$$\bar{\psi}_{\text{ARF}} \equiv \psi_{\text{ARF}}/[\text{ARF}]_T^2.$$

In dimensionless terms, relative rates of transcription and translation can be defined as

$$\begin{aligned}
&\bar{\lambda}_1 \equiv \lambda^{(1)}_{\mathrm{ARF}}/\lambda^{(1)}_{\mathrm{ARF}_2}, \qquad \bar{\lambda}_3 \equiv \lambda_{\text{ARR-Bph}}/\lambda^{(1)}_{\mathrm{ARF}_2}, \qquad \bar{\lambda}_4 \equiv \lambda^{(2)}_{\mathrm{ARF}}/\lambda^{(2)}_{\mathrm{ARF}_2}\\
&\bar{\delta}_{\mathrm{IAA}_p} \equiv \lambda^{(1)}_{\mathrm{ARF}_2}/(\mu_{\mathrm{IAA}_m}[\mathrm{TIR1}^{\ddagger}]_T), \qquad \bar{\delta}_{\mathrm{AR}_p} \equiv \lambda^{(1)}_{\mathrm{ARF}_2}/(\mu_{\mathrm{AR}_m}[\mathrm{TIR1}^{\ddagger}]_T),\\
&\bar{\delta}_{\mathrm{PIN}_p} \equiv \lambda^{(2)}_{\mathrm{ARF}_2}/(\mu_{\mathrm{PIN}_m}[\mathrm{TIR1}^{\ddagger}]_T).
\end{aligned} \tag{A.4}$$

From the above considerations, and dropping the bars, the auxin mediated regulation model becomes

$$\begin{aligned}
&\frac{d[\mathrm{IAA}_m]}{dt} = -[\mathrm{IAA}_m] + \phi_{\mathrm{IAA}_p}\left(\bar{\lambda}_1 F^{(1)}_{\mathrm{ARF}}(t) + F^{(1)}_{\mathrm{ARF}_2}(t) + \bar{\lambda}_3 F^{(1)}_{\text{ARR-Bph}}(t)\right),\\
&\epsilon\frac{[\mathrm{IAA}_p]}{dt} = \delta_{\mathrm{IAA}_p}[\mathrm{IAA}_m] + l_d[\text{Aux:TIR1:IAA}] - l_a[\text{Aux:TIR1}][\mathrm{IAA}_p]\\
&+ \epsilon\eta_{\text{ARF:IAA}}\left(p_d[\text{ARF:IAA}] - p_a[\mathrm{ARF}][\mathrm{IAA}_p]\right),\\
&\epsilon\frac{[\text{Aux:TIR1}]}{dt} = k_a[\mathrm{Aux}][\mathrm{TIR1}] - k_d[\text{Aux:TIR1}] + (l_d+1)[\text{Aux:TIR1:IAA}]\\
&- l_a[\text{Aux:TIR1}][\mathrm{IAA}_p],\\
&\epsilon\frac{[\text{Aux:TIR1:IAA}]}{dt} = l_a[\text{Aux:TIR1}][\mathrm{IAA}_p] - (l_d+1)\,[\text{Aux:TIR1:IAA}],\\
&\epsilon\frac{[\mathrm{IAA}^*]}{dt} = [\text{Aux:TIR1:IAA}] - \mu_{\mathrm{IAA}^*}[\mathrm{IAA}^*],\\
&\frac{[\text{ARF:IAA}]}{dt} = p_a[\mathrm{ARF}][\mathrm{IAA}_p] - p_d[\text{ARF:IAA}],\\
&\frac{[\mathrm{ARF}_2]}{dt} = q_a[\mathrm{ARF}]^2 - q_d[\mathrm{ARF}_2],
\end{aligned} \tag{A.5}$$

$$\epsilon\frac{[\text{Aux}]}{dt} = \epsilon\mu_{\text{Aux}}\left(\alpha_{\text{Aux}} - [\text{Aux}]\right) - \eta_{\text{Aux:TIR1}}\left(k_a[\text{Aux}][\text{TIR1}] - k_d[\text{Aux:TIR1}]\right),$$
$$\frac{[\text{PIN}_m]}{dt} = -[\text{PIN}_m] + \phi_{\text{PIN}_p}\left(\bar{\lambda}_4 F^{(2)}_{\text{ARF}}(t) + F^{(2)}_{\text{ARF}_2}(t)\right),$$
$$\epsilon\tau_{\text{PIN}}\frac{[\text{PIN}_p]}{dt} = \delta_{\text{PIN}_p}[\text{PIN}_m] - [\text{PIN}_p],$$
$$\frac{[\text{AR}_m]}{dt} = -[\text{AR}_m] + \phi_{\text{AR}_p}\left(\bar{\lambda}_4 F^{(2)}_{\text{ARF}}(t) + F^{(2)}_{\text{ARF}_2}(t)\right) - [\text{AR}_m],$$
$$\epsilon\tau_{\text{AR}}\frac{[\text{AR}_p]}{dt} = \delta_{\text{AR}_p}[\text{AR}_m] - [\text{AR}_p],$$

with dimensionless conservation laws

$$\alpha_{\text{TIR1}} = [\text{TIR1}] + [\text{Aux:TIR1}] + [\text{Aux:TIR1:IAA}]$$
$$\alpha_{\text{ARF}} = [\text{ARF}] + [\text{ARF:IAA}] + 2[\text{ARF}_2]$$

and initial conditions equal to zero for all variables except for $[\text{Aux}](0) = 1$. In Tables 3 and 4 we report the default parameter values for the dimensionless auxin submodel A.5.

TABLE 3

TABLE 4

Rescaling of cytokinin submodel

As in the previous section, we define the ratios of the timescale of CR, Ck, and ARR-A proteins degradation to that of gene expression as follows

$$\epsilon_{\text{CR}} \equiv \mu_{\text{CR}_m}/\mu_{\text{CR}_p}, \qquad \epsilon_{\text{Ck}} \equiv \mu_{\text{Ck}_m}/\mu_{\text{Ck}}, \qquad \epsilon_{\text{ARR-A}} \equiv \mu_{\text{ARR-A}_m}/\mu_{\text{ARR-A}}.$$

We then introduce the proportionality constants

$$\tau_{\mathrm{CR}} \equiv \epsilon_{\mathrm{CR}_m}/\epsilon, \qquad \tau_{\mathrm{Ck}} \equiv \epsilon_{\mathrm{Ck}_m}/\epsilon, \qquad \tau_{\text{ARR-A}} \equiv \epsilon_{\text{ARR-A}_m}/\epsilon,$$

and we define the ratio of protein translations with protein degradations as

$$\phi_{\mathrm{CR}_p} \equiv \delta_{\mathrm{CR}_p}/\mu_{\mathrm{CR}_p}, \qquad \phi_{\mathrm{Ck}} \equiv \delta_{\mathrm{Ck}}/\mu_{\mathrm{Ck}}, \qquad \phi_{\text{ARR-A}_p} \equiv \delta_{\text{ARR-A}_p}/\mu_{\text{ARR-A}_p}.$$

We scale mRNA concentrations so that these ratios represent the maximum rate of transcription in the dimensionless system

$$[\overline{\mathrm{CR}_m}] \equiv \frac{\mu_{\mathrm{IAA}_m}\delta_{\mathrm{CR}_p}}{\lambda^{(2)}_{\mathrm{ARF}}\mu_{\mathrm{CR}_p}}[\mathrm{CR}_m], \qquad [\overline{\text{ARR-A}_m}] \equiv \frac{\mu_{\mathrm{IAA}_m}\delta_{\text{ARR-A}_p}}{\lambda_{\mathrm{AR}}\mu_{\text{ARR-A}_p}}[\text{ARR-A}_m].$$

We scale the concentrations of the phosphorylated complexes by a representative total concentration of the phosphoryl group

$$([\overline{\mathrm{AHKph}}], [\overline{\mathrm{Ck{:}AHKph}}]) \equiv ([\mathrm{AHKph}], [\mathrm{Ck{:}AHKph}])/[\mathrm{PH}^{\ddagger}]_T,$$
$$([\overline{\text{ARR-Aph}}], [\overline{\text{ARR-Bph}}]) \equiv ([\text{ARR-Aph}], [\text{ARR-Bph}])/[\mathrm{PH}^{\ddagger}]_T.$$

It is then convenient to scale the concentrations of the other proteins and complexes by the AHK receptor total concentration

$$([\overline{\mathrm{CR}_p}], [\overline{\mathrm{Ck{:}AHK}}]) \equiv ([\mathrm{CR}_p], [\mathrm{Ck{:}AHK}])/[\mathrm{AHK}^{\ddagger}]_T,$$
$$([\overline{\text{ARR-A}_p}], [\overline{\text{ARR-B}_p}]) \equiv ([\text{ARR-A}_p], [\text{ARR-B}_p])/[\mathrm{AHK}^{\ddagger}]_T.$$

We base the concentration of free cytokinin on a representative concentration of cytokinin $[\mathrm{Ck}^{\ddagger}]$

$$[\overline{\mathrm{Ck}}] \equiv [\mathrm{Ck}]/[\mathrm{Ck}^{\ddagger}].$$

These scalings lead to the dimensionless parameters

$$\alpha_{\text{AHK}} \equiv [\text{AHK}]_T/[\text{AHK}^{\ddagger}]_T, \qquad \alpha_{\text{ARR-B}} \equiv [\text{ARR-B}]_T/[\text{AHK}^{\ddagger}]_T,$$
$$\alpha_{\text{Ck}} \equiv \omega_{\text{Ck}}/(\mu_{\text{Ck}}[\text{Ck}^{\ddagger}]), \tag{A.6}$$

and to the definition of the ratios between the total concentrations of the phosphoryl group with cytokinin and AHK receptor total concentrations

$$\eta_{\text{CkPh}} \equiv [\text{PH}^{\ddagger}]_T/[\text{Ck}^{\ddagger}], \qquad \eta_{\text{AHKph}} \equiv [\text{PH}^{\ddagger}]_T/[\text{AHK}^{\ddagger}]_T.$$

We base the association and dissociation constants relative to the phosphoryl group transfer pathway on CR_p degradation

$$\bar{r}_a \equiv (r_a[\text{Ck}^{\ddagger}])/\mu_{\text{CR}_p}, \qquad \bar{r}_d \equiv r_d/\mu_{\text{CR}_p},$$
$$\bar{u}_a \equiv (u_a[\text{AHK}^{\ddagger}]_T)/\mu_{\text{CR}_p}, \qquad \bar{u}_d \equiv (u_d[\text{AHK}^{\ddagger}]_T)/\mu_{\text{CR}_p},$$
$$\bar{s}_a \equiv (s_a[\text{AHK}^{\ddagger}]_T)/\mu_{\text{CR}_p}, \qquad \bar{s}_d \equiv (s_d[\text{AHK}^{\ddagger}]_T)/\mu_{\text{CR}_p}. \tag{A.7}$$

Cytokinin degradation is based on Aux/IAA mRNA degradation

$$\bar{\mu}_{\text{Ck}} \equiv \mu_{\text{Ck}}/\mu_{\text{IAA}_m}.$$

From these scalings, the scaling of the dimensionless protein-DNA binding concentration thresholds follows

$$\bar{\theta}_{\text{ARR-Aph}} \equiv \theta_{\text{ARR-Aph}}/[\text{PH}^{\ddagger}]_T, \qquad \bar{\theta}_{\text{ARR-Bph}} \equiv \theta_{\text{ARR-Bph}}/[\text{PH}^{\ddagger}]_T.$$

Finally, we define the new translation rates as

$$\bar{\delta}_{\text{CR}_p} \equiv \lambda^{(2)}_{\text{ARR-Bph}}/(\mu_m[\text{AHK}^{\ddagger}]_T), \qquad \bar{\delta}_{\text{Ck}} \equiv \lambda^{(1)}_{\text{ARF}_2}/(\mu_m[\text{Ck}^{\ddagger}]_T),$$
$$\bar{\delta}_{\text{ARR-A}_p} \equiv \lambda_{\text{AR}}/(\mu_m[\text{AHK}^{\ddagger}]_T),$$

keeping unchanged the transcription rates. Dropping the bars the cytokinin mediated regulation model becomes

$$\frac{d[\mathrm{CR}_m]}{dt} = \phi_{\mathrm{CR}_p} F^{(2)}_{\text{ARR-Bph}}(t) - [\mathrm{CR}_m],$$
$$\epsilon\tau_{\mathrm{CR}} \frac{d[\mathrm{CR}_p]}{dt} = \delta_{\mathrm{CR}_p}[\mathrm{CR}_m] - [\mathrm{CR}_p],$$
$$\epsilon\tau_{\mathrm{CR}} \frac{d[\text{AHKph}]}{dt} = r_d[\text{Ck:AHKph}] - r_a[\text{AHKph}][\text{Ck}],$$
$$\epsilon\tau_{\mathrm{CR}} \frac{d[\text{Ck}]}{dt} = \epsilon\tau_{\mathrm{CR}}\mu_{\mathrm{Ck}}\left(\alpha_{\mathrm{Ck}} - [\text{Ck}]\right) - \eta_{\mathrm{CkPh}}\left(r_a[\text{AHKph}][\text{Ck}] - r_d[\text{Ck:AHKph}]\right),$$
$$\epsilon\tau_{\mathrm{CR}} \frac{d[\text{ARR-Bph}]}{dt} = u_a[\text{ARR-B}_p][\text{Ck:AHKph}] - u_d[\text{ARR-Bph}][\text{Ck:AHK}],$$
$$\epsilon\tau_{\mathrm{CR}} \frac{d[\text{ARR-Aph}]}{dt} = s_a[\text{ARR-A}_p][\text{Ck:AHKph}] - s_d[\text{ARR-Aph}][\text{Ck:AHK}],$$
$$\frac{d[\text{ARR-A}_m]}{dt} = \phi_{\text{ARR-A}_p} F_{\mathrm{AR}}(t) - [\text{ARR-A}_m],$$
$$\epsilon\tau_{\text{ARR-A}} \frac{[\text{ARR-A}_p]}{dt} = \delta_{\text{ARR-A}_p}[\text{ARR-A}_m] - [\text{ARR-A}_p] + \eta_{\mathrm{AHKph}}(s_d[\text{ARR-Aph}][\text{Ck:AHK}]$$
$$- s_a[\text{ARR-A}_p][\text{Ck:AHKph}]), \tag{A.8}$$

with the associated conservation laws

$$\alpha_{\text{ARR-B}} = [\text{ARR-B}_p] + \eta_{\mathrm{AHKph}}[\text{ARR-Bph}_p],$$
$$\alpha_{PH} = [\text{AHKph}] + [\text{ARR-Aph}] + [\text{ARR-Bph}] + [\text{Ck:AHKph}],$$
$$\alpha_{\mathrm{AHK}} = [\text{Ck:AHK}] + \eta_{\mathrm{AHKph}}([\text{AHKph}] + [\text{Ck:AHKph}]),$$

and initial conditions equal to zero for all variables except for $[\text{AHKph}](0) = 1$ and $[\text{Ck}](0) = 1$. In Table 5 we report the default parameter values for the dimensionless auxin submodel A.8.

TABLE 5

Acknowledgements

The authors thank Leah Band and Alistair Middleton for useful discussions and anonymous referees for constructive criticisms. We gratefully acknowledge the Engineering and Sciences Research Council and the Biotechnology and Biological Research Council for financial support as part of the CISB programme award to CPIB.

References

References

[1] A. Nordström, P. Tarkowski, D. Tarkowska, R. Norbaek, C. Astot, K. Dolezal, G. Sandberg. Auxin regulation of cytokinin biosynthesis in *Arabidopsis thaliana*: A factor of potential importance for auxin-cytokinin regulated development. *PNAS*, Volume 101, no. 21, 8039-8044 (2004).

[2] V.A. Grieneisen, J. Xu, A.F.M. Mare, P. Hogeweg, B. Scheres Auxin transport is sufficient to generate a maximum and gradient guiding root growth *Nature*, Vol. 449, 1008-1013 (2007).

[3] L. Moubayidin, R. Di Mambro, S. Sabatini. Cytokinin-auxin crosstalk. *Trends in Plant Science*, Volume 14, Issue 10, 557-562 (2009).

[4] K. Miyawaki, M. Matsumoto-Kitano, K. Kakimoto. Expression of cytokinin biosynthetic isopentenyltransferase genes in Arabidopsis: tissue specificity and regulation by auxin, cytokinin, and nitrate *The Plant Journal*, 37, 128-138 (2004).

[5] L. Laplaze, E. Benkova, I. Casimiro, L. Maes, S. Vanneste, R. Swarup, D. Weijers, V. Calvo, B. Parizot, M. Begoa Herrera-Rodriguez, R. Offringa, N. Graham, P. Doumas, J. Friml, D. Bogusz, T. Beeckman, M. Bennett. Cytokinins Act Directly on Lateral Root Founder Cells to Inhibit Root Initiation *The Plant Cell* 19:3889-3900 (2007).

[6] M. Laskowski, V.A. Grieneisen, H. Hofhuis, C.A. ten Hove, P. Hogeweg, A.F.M. Mare, B. Scheres Root System Architecture from Coupling Cell Shape to Auxin Transport *PLoS Biology* Vol. 6, Issue 12, e307, (2010)

[7] V.V. Mironova, N.A. Omelyanchuk, G. Yosiphon, S.I. Fadeev, N.A. Kolchanov, E. Mjolsness, V.A. Likhoshvai. A plausible mechanism for auxin patterning along the developing root *BMC Systems Biology* 4:98, 2010

[8] A.M. Middleton, J.R. King, M.J. Bennett, M.R. Owen. Mathematical modelling of the Aux/IAA negative feedback loop. *Bull. Math. Biol.*, 2010 Feb 5. [Epub ahead of print].

[9] I. De Smet, T. Tetsumura, B. De Rybel, N. Frei dit Frey, L. Laplaze, I. Casimiro, R. Swarup, M. Naudts, S. Vanneste, D. Audenaert, D. Inz, M. Bennett, T. Beeckman. Auxin-dependent regulation of lateral root positioning in the basal meristem of Arabidopsis. *Development*, 134(4):681, 2007.

[10] B. Péret, B. De Rybel, I. Casimiro, E. Benkov, R. Swarup, L. Laplaze, T. Beeckman, M. Bennett. *Arabidopsis* lateral root development: an emerging story. *Trends in Plant Science*, Volume 14, Issue 7, 399-408, (2009)

[11] E. Benková, M. Michniewicz, M. Sauer, T. Teichmann, D. Seifertová, J.G. Friml. Local, efflux-dependent auxin gradients as a common module for plant organ formation. *Cell*, 115:591-602, 2003.

[12] M.A. Moreno-Risueno, J.M. Van Norman, A. Moreno, J. Zhang, S.E. Ahnert, P.N. Benfey. Oscillating Gene Expression Determines Competence for Periodic *Arabidopsis* Root Branching. *Science*, Volume 329, 1306, (2010).

[13] J. Traas, T. Vernoux. Oscillating Roots. *Science*, Volume 329, 1290 (2010)

[14] G. Hagen, T. Guilfoyle. Auxin-responsive gene expression: genes, promoters and regulatory factors. *Plant Mol. Biol.*, 49, 373-385 (2002).

[15] T. Ulmasov, G. Hagen, T. Guilfoyle. Dimerization and DNA binding of auxin response factors. *The Plant Journal*, 19(3), 309-319, (1999).

[29] T. Guilfoyle, G. Hagen, T. Ulmasov, J. Murfett. How does auxin turn on genes? *Plant Physiol.*, 118, 341-347 (1998).

[30] S.B. Tiwari, G. Hagen, T. Guilfoyle. The roles of Auxin response factor domains in Auxin-responsive transcription. *Plant Cell*, 15, 533-543 (2003).

[18] W.M. Gray, S. Kepinski, D. Rouse, O. Leyser, M. Estelle. Auxin regulates SCF(TIR1)-dependent degradation of AUX/IAA proteins. *Nature*, 414, 271 (2001).

[19] S. Kepinski, O. Leyser The arabidopsis f-box protein tir1 is an auxin receptor. *Nature*, 435,436-437 (2005).

[20] N. Zenser, A. Ellsmore, C. Leasure, J. Callis. Auxin modulates the degradation rate of Aux/IAA proteins. *Proc. Natl. Acad. Sci.* USA 98, 11795-117800 (2001).

[21] J. Lewis. Autoinhibition with Transcriptional Delay: A Simple Mechanism for the Zebrafish Somitogenesis Oscillator *Current Biology*, Vol. 13, 13981408, (2003).

[22] N.A.M. Monk. Oscillatory expression of Hes1, p53, and NF-kB driven by transcriptional time delays. *Current Biology*, Vol. 13, 14091413, (2003).

[23] B. Jones, S. Andersson Gunners, S. V. Petersson, P. Tarkowski, N. Graham, S. May, K. Dolezal, G. Sandberg, K. Ljung Cytokinin Regulation of Auxin Synthesis in Arabidopsis Involves a Homeostatic Feedback Loop Regulated via Auxin and Cytokinin Signal Transduction. *Plant Cell.* 2010 Sep 7. [Epub ahead of print]

[24] R. Dello Ioio, K. Nakamura, L. Moubayidin, S. Perilli, M. Taniguchi, M.T. Morita, T. Aoyama, P. Costantino, S. Sabatini. A Genetic Framework for the Control of Cell Division and Differentiation in the Root Meristem. *Science*, 322:1380-1384, 2008.

[25] S. Dharmasisi, M. Estelle. The role of regulated protein degradation in auxin response. *Plant Mol. Biol.*, 49, 401409 (2002).

[26] W.D. Teale, I.A. Paponov, K. Palme. Auxin in action: signalling, transport and the control of plant growth and development. *Nat. Rev. Mol. Cell Biol.*, 7, 847859 (2006).

[27] E.M. Kramer, M.J. Bennett. Auxin transport: a field in flux. *Trends Plant Sci.*, 11:382-386 (2006).

[28] A. Imamura, T. Kiba, Y. Tajima, T. Yamashino, T. Mizuno. In Vivo and In Vitro Characterization of the ARR11 Response Regulator Implicated in the His-to-Asp Phosphorelay Signal Transduction in *Arabidopsis thaliana Plant Cell Physiol.*, 44(2), 122-131 (2003).

[29] T. Guilfoyle, G. Hagen, T. Ulmasov, J. Murfett. How does auxin turn on genes? *Plant Physiol.*, 118, 341347.

[30] S.B. Tiwari, G. Hagan, T. Guilfoyle. The roles of Auxin response factor domains in Auxin responsive transcription. *Plant Cell*, 15, 533543 (2003).

[31] Y. Kuznetsov. Elements of Applied Bifurcation Theory. *Springer-Verlag, New York, 1995,1998, 2004 Science Press, Beijing, 2010.*

[32] B. Ermentrout. Simulating, Analyzing, and Animating Dynamical Systems: A Guide to XPPAUT for Researchers and Students. *SIAM, Philadelphia, 2002.*

[33] S. Abel, M.D. Nguyen, A. Theologis. The PS-IAA4/5-like family of early auxin-inducible mRNAs in Arabidopsis thaliana. *J. Mol. Biol.*, 251:533-549, 1995.

[34] K. Knox, C.S. Grierson, O. Leyser. AXR3 and SHY2 interact to regulate root hair development. *Development*, 130:5769-5777, 2003.

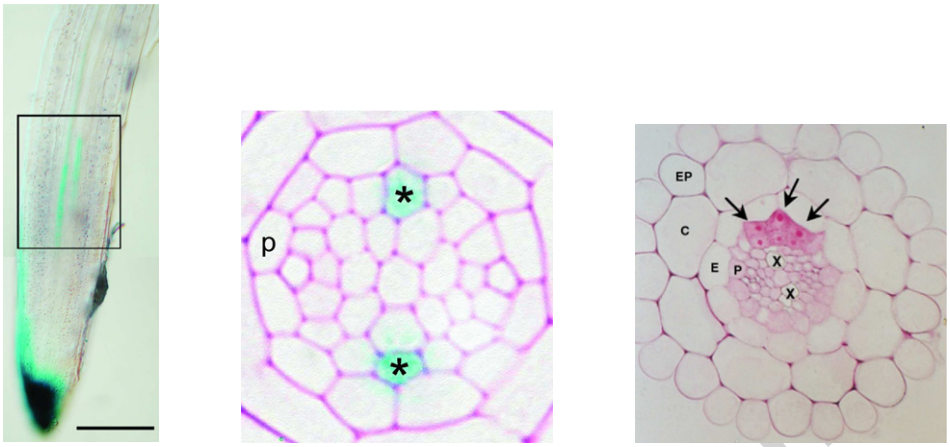

(a) (b) (c)

Figure 1 – *Longitudinal and transverse sections of the Arabidopsis primary root.* (a) DR5::GUS expression in apical part of root grown on MS medium for 40 HAG. (b) Transverse section through the basal meristem of seedling roots expressing DR5::GUS. (c) Three radially expanded pericycle cells have undergone divisions (arrows). Abbreviations: C, cortex; E, endodermis; EP, epidermis; P, pericycle; X, xylem. These figures are reproduced from [1,2].

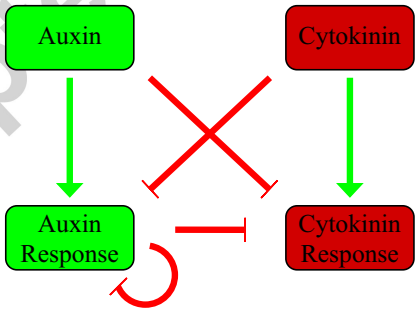

Figure 2 – *Cytokinin-auxin cross-regulation.* Cytokinin and auxin activate the transcription of their own response genes, and repress those of their antagonist. The auxin response is coordinated by the Aux/IAA negative feedback loop and represses the cytokinin response.

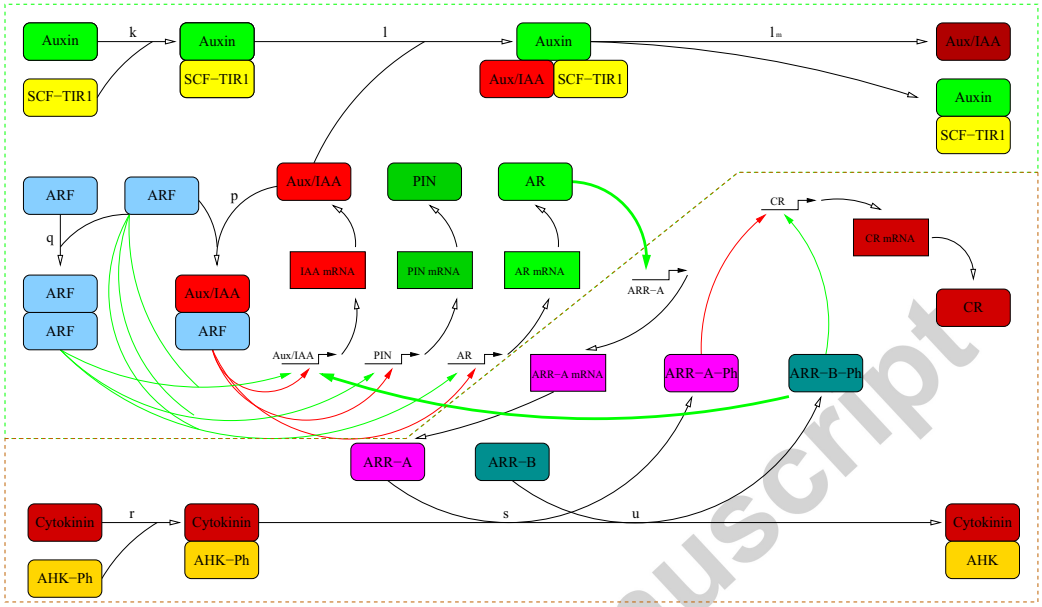

Figure 3 – *Schematic diagram of our cytokinin-auxin signalling network.* The green dashed box contains the auxin mediated regulation of Aux/IAA negative feedback loop as examined in [3]. Auxin binds to SCF-TIR1 and the complex they form targets Aux/IAA protein for ubiquitination. Free ARFs can homodimerise and heterodimerise with the Aux/IAA protein. ARF monomer and homodimer activate the transcription of Aux/IAA, PIN, and auxin response genes. By contrast, the heterodimer represses the transcription of the same genes. An unidentified signalling mechanism dependent on auxin response activates ARR-A, interacting with the cytokinin pathway. The brown dashed box contains cytokinin perception and response activation by phosphorylation. Cytokinin binds to a AHK receptor and the complex they form transfers the phosphoryl group to type A and type B ARRs (ARR-A-Ph and ARR-B-Ph). ARR-A-Ph and ARR-B-Ph then respectively activate and repress cytokinin-regulated genes. ARR-B-Ph also stimulates Aux/IAA transcription, inhibiting auxin-mediated regulation. The coupling between the two hormones can be summarised as follows and is represented in the figure with bold arrows. The auxin response negatively controls the cytokinin response by the activation of ARR-A genes. The cytokinin-mediated phosphorylation of ARR-B transcription factors enhances Aux/IAA transcription, and so balances the auxin response.

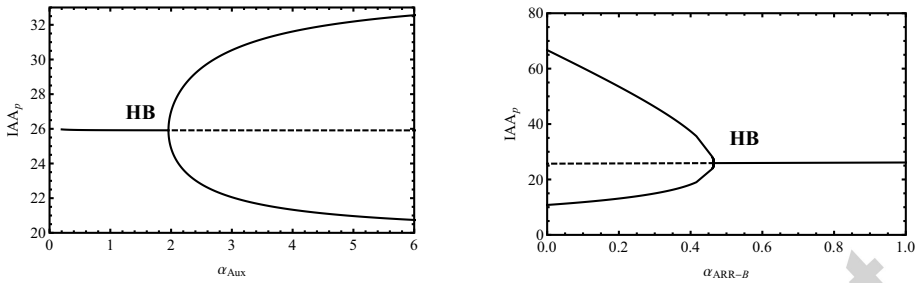

(a) **(b)**

Figure 4 – *Bifurcation diagrams of IAA_p against α_{Aux} and against $\alpha_{ARR\text{-}B}$.* Two supercritical Hopf bifurcations occur, leading the system from a stable steady state to a stable limit cycle, on an increase of α_{Aux}, (a), and a decrease of $\alpha_{\text{ARR-B}}$, (b). Therefore, the range of parameters that generates oscillatory solutions depends on auxin and cytokinin regulation. The bifurcation due to auxin regulation is a direct effect of the increase of auxin supply, whereas cytokinin is indirectly responsible for the bifurcation by triggering the phosphorylation of ARR-B. Here $\alpha_{\text{ARR-B}} = 0.5$; all the other parameter values and the initial conditions are listed in the Appendix.

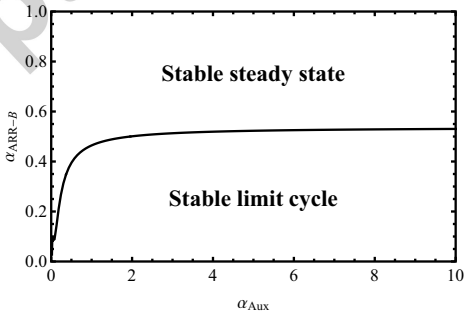

Figure 5 – *Two parameters bifurcation diagram of $\alpha_{ARR\text{-}B}$ against α_{Aux}.* The solid line corresponds to a Hopf-bifurcation. All the parameter values and the initial conditions are listed in the Appendix.

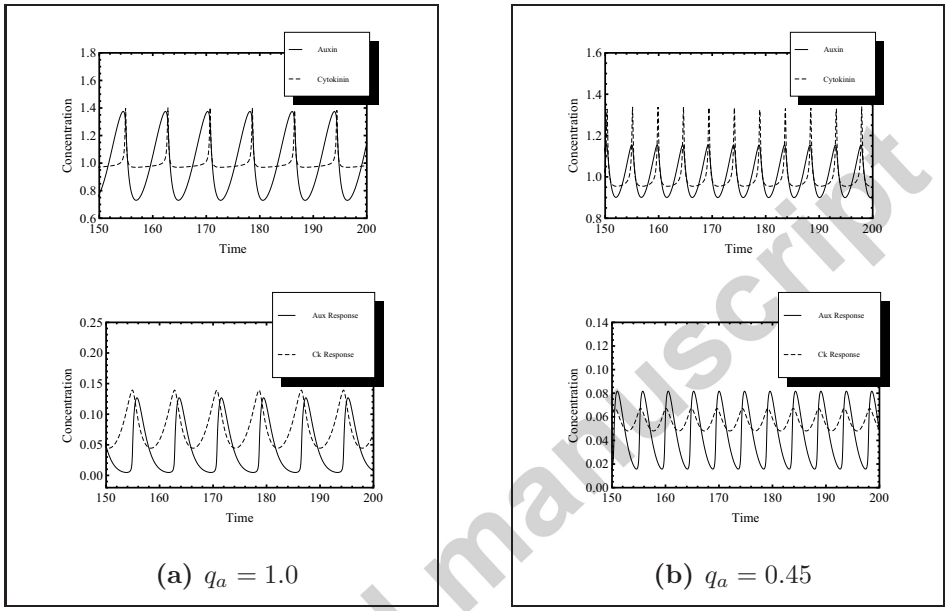

Figure 6 – *The influence of ARF dimerization on auxin and cytokinin.* Limit cycle solutions of auxin, cytokinin, auxin response (AR), cytokinin response (CR), for the ARF dimerization parameter $q_a = 1$, (a), and $q_a = 0.45$, (b). In the pictures above auxin and cytokinin oscillations, in the ones below auxin response (AR) and cytokinin response (CR) periodic solutions. We represent in solid lines auxin and auxin response, in dashed lines cytokinin and cytokinin response. Decreasing the dimerization of the ARFs reduces the phase delay, while the amplitudes of auxin and cytokinin oscillations respectively increase and decrease. The parameter values are $\lambda_{\text{ARR-Bph}} = 0.01, l_a = 10, l_d = 1, k_a = 1, \alpha_{\text{AHK}} = 10, \alpha_{\text{PH}} = 10, \phi_{\text{AR}_p} = 4.5$; all the other parameter values and the initial conditions are listed in the Appendix.

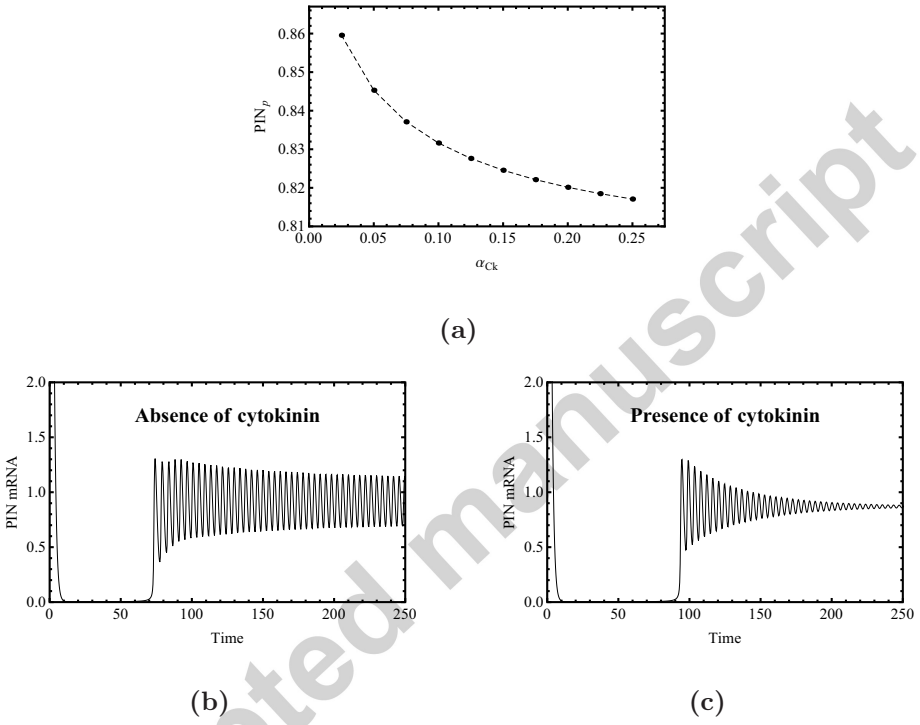

Figure 7 – *PIN dynamics.* (a) An increase in cytokinin supply triggers a decrease in PIN expression, as shown experimentally in [4]. (b) in the absence of cytokinin, we observe oscillations in PIN mRNA levels. (c) following application of cytokinin, after an initial transient period in which PIN mRNA levels are repressed, the system settles via damped oscillations to a stable steady state. Parameter values: In (a) $\alpha_{\text{ARR-B}} = 5$, in (b) $\alpha_{\text{ARR-B}} = 2$, $\alpha_{\text{Ck}} = 0$, and in (c) $\alpha_{\text{ARR-B}} = 2$, $\alpha_{\text{Ck}} = 1$; all other parameter values and the initial conditions are listed in Tables 3 and 4.

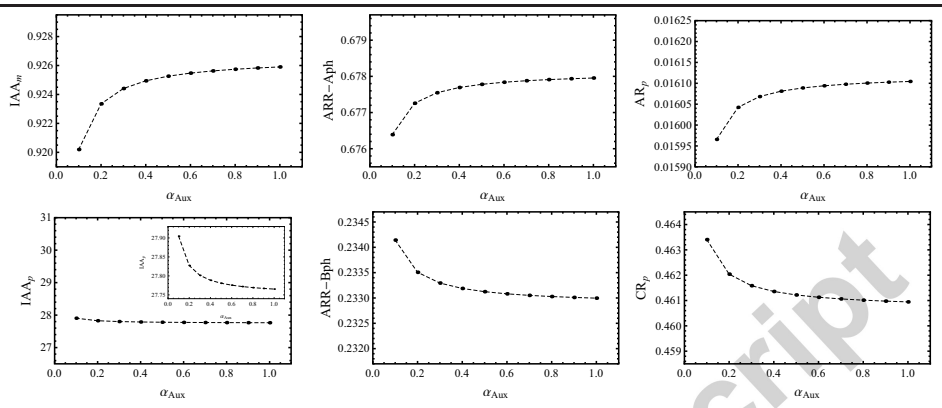

(a) Steady states plotted against α_{Aux}

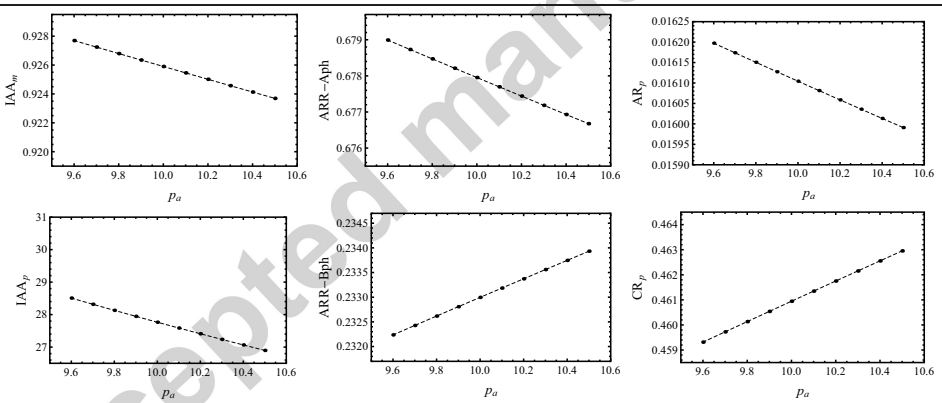

(b) Steady states plotted against p_a

Figure 8 – *Aux/IAA loss of function mutant mimics auxin application.* Series of plots showing how the steady state profiles vary with α_{Aux}, (a), and the association constant p_a, (b). A reduction of p_a mimics an increase in α_{Aux} on the responses of auxin and cytokinin. On the other hand, increased application of auxin degrades IAA$_p$ while the loss-of-function mutant tends to increase IAA$_p$ concentration. $\alpha_{\text{ARR-B}} = 5.$, all the other parameter values and the initial conditions are listed in the Appendix

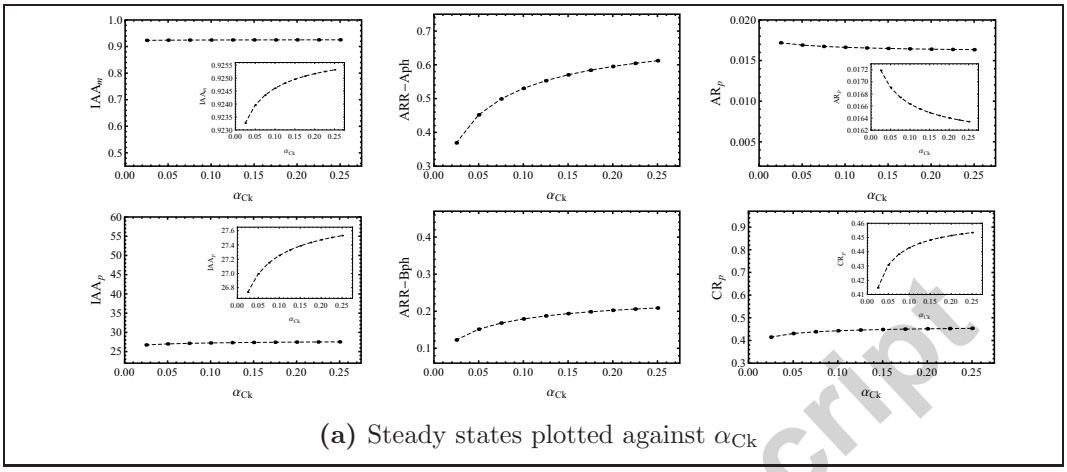

(a) Steady states plotted against α_{Ck}

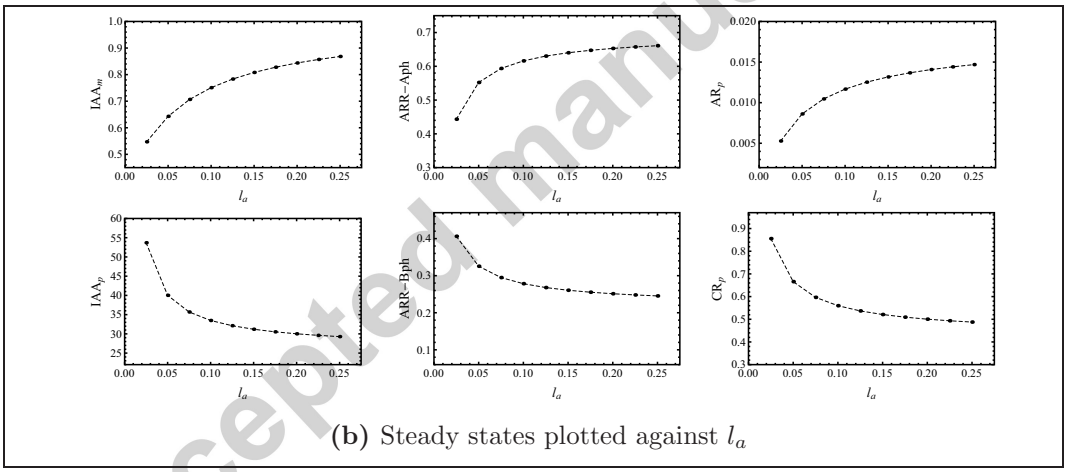

(b) Steady states plotted against l_a

Figure 9 – *Aux/IAA gain of function mutant mimics cytokinin application.* Series of plots showing how the steady state profiles vary with (α_{Ck}), (a), and the association constant l_a, (b). A reduction in l_a mimics an increase α_{Ck} on the responses of auxin and cytokinin. On the other hand, an increased application of cytokinin strengthen IAA_m transcription while, decreasing l_a, IAA_m concentration is reduced. Moreover, the phosphorylated ARR-A concentration is enhanced by cytokinin supply, but is suppressed by the gain-of-function mutant. $\alpha_{\text{ARR-B}} = 5.$, all the other parameter values and the initial conditions are listed in the Appendix.

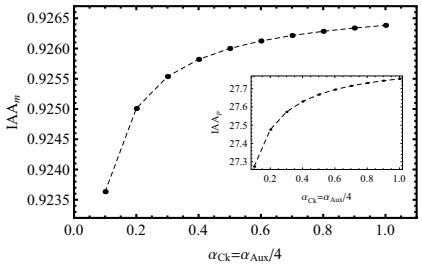

(a) Aux/IAA steady states for constant $\alpha_{\mathrm{Aux}}/\alpha_{\mathrm{Ck}}$

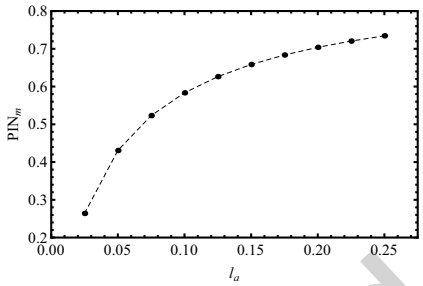

(b) PIN steady states plotted against l_a

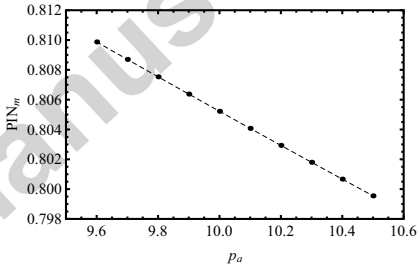

(c) PIN steady states plotted against p_a

Figure 10 – *(a): Aux/IAA steady-state solutions for constant α_{Aux}/α_{Ck}.* Steady-state solutions of Aux/IAA mRNA as the supply of cytokinin (α_{Ck}) and of auxin (α_{Aux}) vary by keeping a constant auxin-to-cytokinin supply ratio. An increase in cytokinin supply triggers an increase in Aux/IAA expression, although the hormonal concentration ratio is not varied. *(b) and (c): PIN response to Aux/IAA gain- and loss-of-function mutants.* PIN mRNA steady states concentrations plotted against the association constants l_a, (b), and p_a, (c). PIN mRNA levels decrease as l_a decreases, and increase as p_a decreases. The gain- and loss-of-function mutants respectively promote and weaken PIN transcription. $\alpha_{\mathrm{ARR\text{-}B}} = 5.$, all the other parameter values and the initial conditions are listed in the Appendix.

Species concentration	Species name	Species type
$[IAA_m]$	Aux/IAA	mRNA
$[IAA_p]$	Aux/IAA	Protein
[TIR1]	SCF-TIR1	Receptor
[Aux:TIR1]	auxin-SCF-TIR1	Hormone-receptor complex
[Aux:TIR1:IAA]	auxin-SCF-TIR1-Aux/IAA	Oligomer complex
$[IAA^*]$	Tagged Aux/IAA	Protein
[ARF]	ARF monomer	Transcription factor
[ARF:IAA]	ARF-Aux/IAA heterodimer	Transcription factor complex
$[ARF_2]$	ARF homodimer	ARF homodimer
[Aux]	auxin	Hormone
$[PIN_m]$	PIN	mRNA
$[PIN_p]$	PIN	Protein
$[AR_m]$	auxin response	mRNA
$[AR_p]$	auxin response	Protein

Table 1: *Table summarising the species involved in auxin regulation.*

Species concentration	Species name	Species type
[CR_m]	cytokinin response	mRNA
[CR_p]	cytokinin response	Protein
[AHKph]	AHK	Receptor+phosphoryl group
[Ck]	cytokinin	Hormone
[Ck:AHK]	cytokinin-AHK	Hormone-receptor complex
[Ck:AHKph]	cytokinin-AHK	Hormone-receptor complex+phosphoryl group
[ARR-A_m]	type A ARR	mRNA
[ARR-A_p]	type A ARR	Protein
[ARR-Aph]	type A ARR	Protein+phosphoryl group
[ARR-B_p]	type B ARR	Protein
[ARR-Bph]	type B ARR	Protein+phosphoryl group

Table 2: *Table summarising the species involved in cytokinin regulation.*

Parameter	Dimensionless value	Parameter description
ϵ	0.01	Aux/IAA transcription degradation ratio
$\bar{\lambda}_1$	0.1	ARF relative transcription rate
$\bar{\lambda}_3$	0.02	ARR-Bph relative transcription rate
α_{Aux}	1	Auxin supply
α_{TIR1}	1	TIR1 relative concentration
α_{ARF}	1	ARF relative concentration
ϕ_{IAAp}	100	Aux/IAA translation/degradation ratio
ϕ_{ARp}	2	AR translation/degradation ratio
ϕ_{PINp}	100	PIN translation/degradation ratio
δ_{IAAp}	1	Aux/IAA translation rate
δ_{ARp}	1	AR translation rate
δ_{PINp}	1	PIN translation rate
μ_{Aux}	0.1	Auxin degradation rate
μ_{IAAs}	1	Aux/IAA degradation rate
$\eta_{\mathrm{Aux:TIR1}}$	10	TIR1/auxin concentration ratio
$\eta_{\mathrm{ARF:IAA}}$	1	ARF/TIR1 concentration ratio

Table 3: *Default values of dimensionless parameters for the auxin submodel described in the Appendix (part 1/2).*

Parameter	Dimensionless value	Parameter description
l_a	0.5	Relative association rate
l_d	0.1	Relative dissociation rate
p_a	10	Relative association rate
p_d	10	Relative dissociation rate
k_a	100	Relative association rate
k_d	1	Relative dissociation rate
q_a	1	Relative association rate
q_d	1	Relative dissociation rate
θ_{ARF}	0.1	Protein/DNA binding rate
θ_{ARF2}	0.01	Protein/DNA binding rate
$\theta_{\mathrm{ARF:IAA}}$	0.1	Protein/DNA binding rate
θ_{IAAp}	0.1	Protein/DNA binding rate
θ_{ARp}	0.1	Protein/DNA binding rate
$\psi_{\mathrm{ARF:IAA}}$	0.1	Protein/DNA binding rate
ψ_{ARF}	0.1	Protein/DNA binding rate
τ_{PIN}	1	Proportionality constant
τ_{AR}	1	Proportionality constant

Table 4: *Default values of dimensionless parameters for the auxin submodel described in the Appendix (part 2/2).*

Parameter	Dimensionless value	Parameter description
α_{Ck}	1	Cytokinin supply
$\alpha_{\text{ARR-B}}$	1	ARR-B relative concentration
α_{AHK}	1	AHK relative concentration
α_{PH}	1	PH relative concentration
ϕ_{CRp}	2	CR translation/degradation ratio
$\phi_{\text{ARR-Ap}}$	100	ARR-A translation/degradation ratio
δ_{CRp}	1	CR translation rate
$\delta_{\text{ARR-Ap}}$	1	ARR-A translation rate
μ_{Ck}	0.1	Cytokinin degradation rate
η_{AHKph}	1	PH/AHK concentration ratio
η_{CkPh}	1	PH/cytokinin concentation ratio
r_a	1	Relative association rate
r_d	1	Relative dissociation rate
u_a	1	Relative association rate
u_d	1	Relative dissociation rate
s_a	1	Relative association rate
s_d	1	Relative dissociation rate
$\theta_{\text{ARR-Aph}}$	0.1	Protein/DNA binding rate
$\theta_{\text{ARR-Bph}}$	0.1	Protein/DNA binding rate
τ_{CR}	1	Proportionality constant
$\tau_{\text{ARR-A}}$	1	Proportionality constant

Table 5: *Default values of dimensionless parameters for the cytokinin submodel described in the Appendix.*

HIGHLIGHTS

1) We model the cross-talk between auxin and cytokinin during root development.

2) We analyse the response of their signaling network to mutations and hormonal perturbations.

3) We show that some elements of the network respond differently in these two cases.

4) We show that an analysis based on hormonal ratio may be misleading.

5) We conclude that this mathematical model can stimulate further experimental work.